Fine Chemical Engineering
http://ojs.wiserpub.com/index.php/FCE/

Research Article

Artificial Photosynthesis: Visible Light-Activated $TiOCl_2$/2-Phenyl Indole Complexes for Atmospheric CO_2 and H_2O Capture and Long-Chain Organic Products Generation

Michail Paraskevas[1], **Gregory G. Arzoumanidis**[2*]

[1]Guandong Technion Israel Institute of Technology, Jinping, Shantou, Guandong 515063, P. R. China
[2]Oakwood Consulting, Inc. Naperville, IL 60540, USA
E-mail: arzoumandis@gmail.com

Received: 9 April 2024; **Revised:** 26 July 2024; **Accepted:** 30 July 2024

Abstract: We present a novel self-organized chemical "living" system that mimics natural photosynthesis by capturing CO_2 and H_2O from the atmosphere at ambient conditions. This system autonomously reduces CO_2 with H_2O protons to produce long-chain aliphatic oxygenated products. Starting with 2-phenyl indole (PI) complexes with $TiCl_4$, the hydrolyzed complexes react with CO_2 to form organotitanium carbonates. The 2:1 PI/$TiCl_4$ complex was found to be the most effective. Key findings include: **Photocatalytic Reduction:** Visible light reduces Ti^{IV} to Ti^{III} and Ti^{II}, forming peroxotitanium complexes and releasing OH radicals. **CO_2 Reduction:** CO_2 is reduced to CO, H_2CO, and CH_3OH, which couple to form $HOCH_2CH_2OH$. **Organic Compound Synthesis:** The system generates oxygenated organic compounds with carbon chains from C_2 to C_{16}. **Ligand Exchange:** The PI ligand exchanges with donor molecules, forming adducts involved in the photocatalytic process. **PI Oligomerization:** Contributes to the formation of PI oligomers. These processes were monitored using matrix-assisted laser desorption/ionization-time of flight (MALDI-TOF) spectra, proton and Carbon-13 nuclear magnetic resonance (^{13}C NMR), and infrared (IR) spectra, identifying over two dozen intermediates and products. This system offers a prototype for new applications with potential improvements using other metals and ligands.

Graphical abstract:

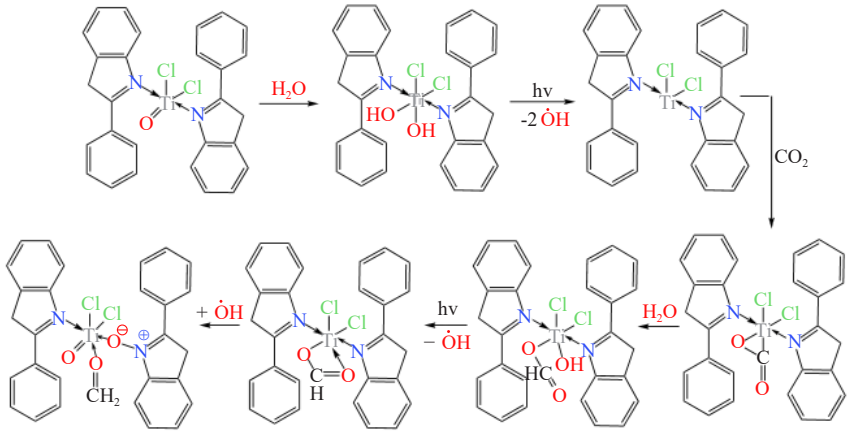

DOI: https://doi.org/10.37256/fce.5220244715

***Keywords*:** photosynthesis, organotitanium, CO_2 and H_2O capture, CO_2 reduction, living chemical system, photocatalysis, OH radicals, photosynthetic products

1. Introduction

"Living" chemical systems "can harvest energy to move autonomously and self-organize to perform complex tasks".[1] Preferred systems are catalysts that operate away from equilibrium, continuously supplied with energy and materials from inexhaustible sources such as sunlight, air, and water. This concept underpins artificial photosynthesis (AP),[2] which currently focuses on water splitting catalyzed mostly by metal oxide semiconductors to produce hydrogen and oxygen, a vibrant research area worldwide. However, AP lacks the second critical characteristic of natural photosynthesis: the autonomous reduction of CO_2 to carbohydrates or other desirable organic materials. Developing an effective "living" photocatalytic system that mimics natural photosynthesis, such as the one reported here, offers immense benefits for environmental protection, energy sufficiency, and sustainability.

Numerous studies report direct sunlight-driven catalytic splitting of water to produce "green" hydrogen and oxygen,[3] often leveraging the catalytic effects of TiO_2 in its various allotropic forms. Although improvements are necessary for commercial viability, the indirect approach of generating hydrogen via electrolysis using solar electricity remains more efficient.[4]

Direct air capture (DAC) of CO_2 from the atmosphere[5] is being actively pursued on an industrial scale to reduce the carbon footprint, though it remains energy-intensive and relies on reactants like KOH, CaO, and amines. To our knowledge, no known system other than natural photosynthesis[6] can capture atmospheric CO_2 and subsequently reduce it autonomously. Current catalytic processes for CO_2 reduction[2] often utilize CO_2 in pure or concentrated forms, with the lowest reported concentration[6] being 0.5%, which is significantly higher than atmospheric levels. A desirable system would combine hydrogen transfer from catalytic water splitting with atmospheric CO_2 reduction to produce targeted organic compounds, moving beyond commonly reported products like CO, HCOOH, HO_2CCO_2H, CH_2O, CH_3OH, C_2H_5OH, C_2H_4, or CH_4.

Many systems for CO_2 reduction require specialized devices (e.g., electrocatalysis, photoelectro-catalysis), high temperatures (thermocatalysis), or demanding preparation procedures (photoelectro-enzyme and/or photoenzyme catalysis), often affecting reproducibility. A relatively simple and reproducible system is more effective, especially for future scale-up.

Since TiO_2 was first reported[7] as a photocatalyst in 1977, it has dominated photocatalysis research due to its excellent optical and electronic properties, high chemical stability, low cost, non-toxicity, and eco-friendliness. TiO_2 in its allotropic forms (rutile, brookite, anatase) has been widely utilized in various forms and methods, either alone or combined with other metals (Fe, Re, Cu, Zn, Pt, Ru) or non-metallic catalysts, for photocatalytic water splitting[8] and CO_2 reduction.[9] Careful design of particle morphology and control of surface chemistry can enhance TiO_2's catalytic activity.[10]

TiO_2's catalytic outcomes are primarily recorded at the bulk level of oxytitanium scaffolds. However, functionalities at the atomic level, such as Ti-O-O,[11] TiO(OH),[12] or $Ti(OH)_2$,[13] enhance photocatalytic performance. These functionalities derive from discrete titanium-oxygen double bonds (Ti=O or $Ti^{\delta+}=O^{\delta-}$)[14] by oxidation and/or hydrolysis, prevalent on the TiO_2 surface. Unlike single molecule photocatalysts[14] like Ru, Co, Mn, and other metal pincer complexes, limited information exists on analogous titanium complexes acting as photocatalysts at the molecular level. One notable exception is the substituted ansa-titanocene dihydroxido complex investigated by Beweries and coworkers[15] shown in Figure 1.

This complex induces OH radical formation under visible light irradiation, with concomitant Ti^{IV} reduction to Ti^{III}, a form of ligand-to-metal charge transfer (LMCT) photochemistry also observed in other 3d metals and used for sustainable organic synthesis.[16] Titanium oxide phthalocyanine (TiOPc) also serves as a molecular photocatalyst, used as a light-sensitive substrate for photoelectronic chips.[17]

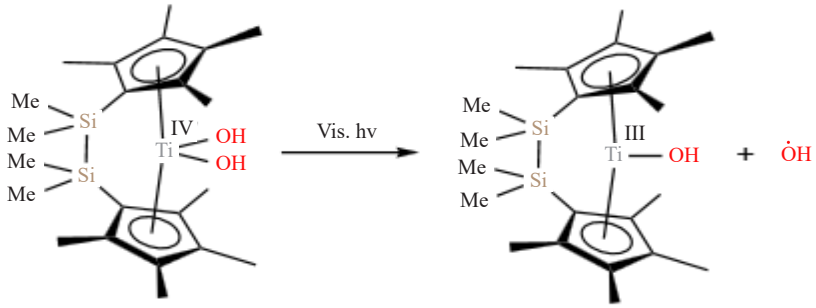

Figure 1. Visible-light OH radicals release from an ansa-titanocene dihydroxido complex. Reduction of Ti^{IV} to Ti^{III}

Recognizing the significance of titanium-oxygen double bonds (Ti=O) and the dihydroxy $Ti(OH)_2$ and peroxo Ti-O-O moieties in photocatalysis at the molecular level opens new, largely unexplored opportunities. Complexation of easily accessible X_2M=O compounds (X = halogen or pseudohalogen, M = Ti, Zr, Hf, V, with titanium oxide dichloride[18] Cl_2Ti=O as a model derivative) combined with photosensitive ligands or other light-sensitive chromophores presents new possibilities.

Complexes of Cl_2Ti=O with nitrogen- or oxygen-donor ligands (e.g., methyl cyanide, trimethylamine, tetrahydrofuran, pyridine, α-picoline, 2-2'-bipyridyl) have been known since the 1960s. Only $TiOCl_2 \cdot 2$(α-picoline) and $TiOCl_2 \cdot 2NMe_3$ indicate the existence of a terminal Ti=O bond in monomeric structures, as shown by IR spectra.[19] In other cases, polymeric structures prevail, with repeating units, as depicted in Figure 2.

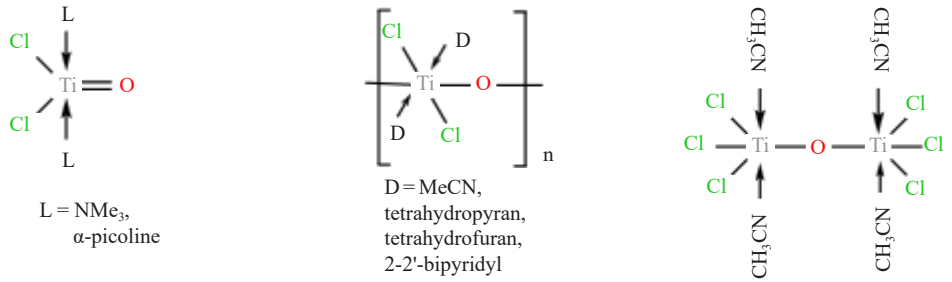

Figure 2. Complexation of $TiOCl_2$ with several small donor molecules

Partial hydrolysis of $TiCl_4 \cdot 2CH_3CN$ yields the Ti-O-Ti derivative as the initial product.[20] Remarkably, pyridine as a ligand for $TiOCl_2$ promotes a polymeric structure, while 2-methyl pyridine (α-picoline) yields a monomeric structure. Steric and electronic factors determine whether a monomeric or polymeric structure forms. However, further hydrolysis of both structures ultimately yields the same dihydroxido complex, $L_2Cl_2Ti(OH)_2$, expected to possess photocatalytic properties akin to the Beweries complex.[15]

2. Results and discussion

Our photocatalytic systems derive from ambient visible light and air exposure of previously reported organotitanium complexes,[21] synthesized by mixing 2-phenyl indole (PI) and $TiCl_4$ in toluene at targeted molar ratios, under a N_2 inert atmosphere. Initially, the 1:1 molar ratio complex **4** rapidly isomerizes to the thermodynamically favored indolenine form **5**, which has a lower DFT-calculated energy than **4** ($\Delta H°$ = -6.9 kcal/mol, $\Delta G°$ = -7.1 kcal/

mol)[22] (Figure 3). Details of the study are provided in Arzoumandis and Chamot[22] under the heading "Density Functional Study of the Ortho-Metalation of 2-Phenyl Indole". Similarly, indole converts to the indolenine form when coordinated with $PdCl_2$.[23]

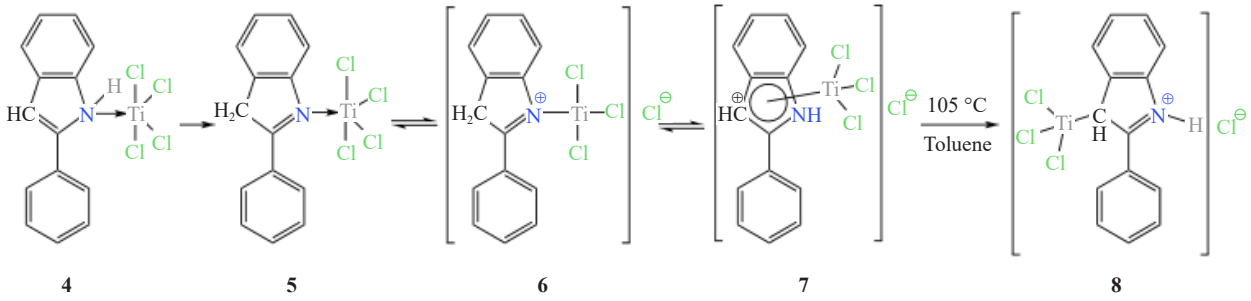

4 **5** **6** **7** **8**

Figure 3. Tautomeric forms of the 1:1 PI:$TiCl_4$ complex (**4**-**7**) with the thermal reaction product **8**

Complex **5** exists in equilibrium with tautomeric forms **6** and **7**, which at elevated temperatures undergo titanation at the 3-position of the indole scaffold.

Mixing PI and $TiCl_4$ at a 1:2 molar ratio in toluene forms the ionic complex **9**, which upon heating the solution to 105 °C precipitates as organometallic complex **10**, sharing the same cation as complex **8** (Figure 4).

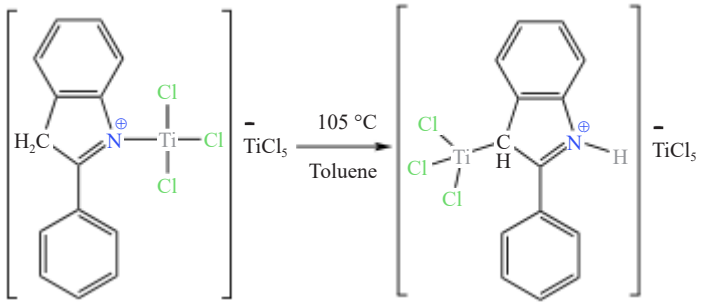

9 **10**

Figure 4. The 1:2 PI:$TiCl_4$ complex **9** with the thermal reaction product **10**, having the same cation as complex **8**

At a 2:1 PI:$TiCl_4$ molar ratio, complex **11** forms, possessing a bi-pyramidal structure. Thermal rearrangement of the hexa-coordinated complex **11** results in the formation of the ortho-metalated complex **12**, with retention of HCl and formation of a hydrogen bond with one of the chlorides attached to Ti, following expulsion of an unreacted PI molecule. Complex **12** is also expected to form from the mixed PI·THF·$TiCl_4$ complex **13** (Figure 5).

Each of the described PI/$TiCl_4$ complexes (**4** through **13**) becomes an active photocatalyst once one or two Ti-Cl bonds transform into Ti-OH, Ti=O, or Ti-O-Ti functionalities through partial hydrolysis, performed by air humidity. The oxotitanium functionalities are responsible for the photocatalytic properties of the complexes, in cooperation with the inherent photoionization potential of the PI non-innocent ligand.[24-27] Indeed, indole and TiO_2 have proven to be a winning photocatalytic combination.[28] None of the complexes in Figure 2, with non-photoactive ligands, have ever been mentioned as photocatalysts. The chemistry described in this paper can be conveniently expanded by substituting PI with other known photoactive ligands currently applied to other metals, such as Ru.[29]

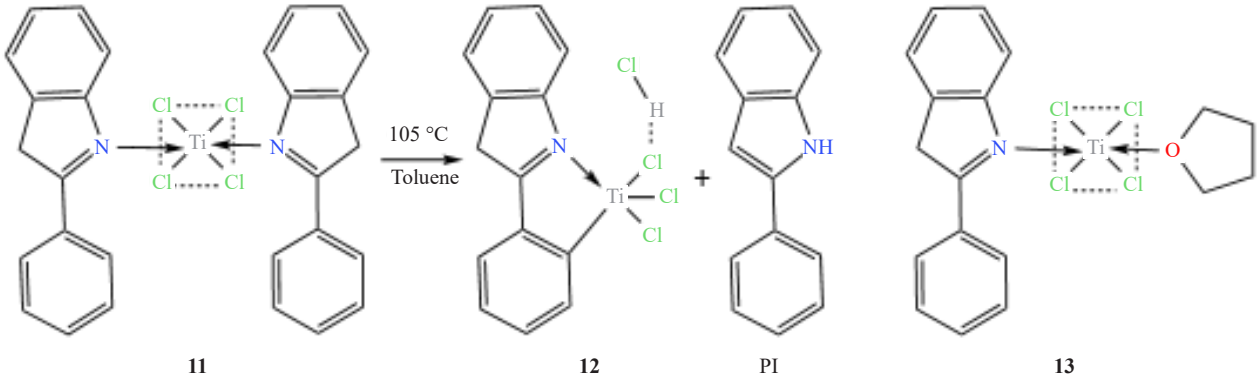

Figure 5. The 2:1 PI:$TiCl_4$ complex **11**, with the ortho-metalated thermal reaction product **12**. The mixed PI·THF·$TiCl_4$ complex **13** could replace complex **11** in the thermal reaction

Our study was prompted by observing a curious color change in complex **11**, upon filtration in open air and subsequent transfer into a glass vial. The tightly closed vial was exposed to room light at ambient temperature for about three weeks. Scattered and uneven color changes from dark brown to khaki and partially green were seen in various areas of the sample bulk, resembling mold growth (see Figure 6). It was remarkable that these color changes occurred in the closed environment of the vial under room light, most likely influenced by the previous exposure of complex **11** to open air as well as by the existing air within the vial.

The dynamic behavior of the complex described above was unexpectedly and revealingly elucidated by four matrix-assisted laser desorption/ionization-time of flight mass spectrometry (MALDI-TOF MS) spectra. Three samples were dissolved in tetrahydrofuran (THF; Figures 7, 8, 9) and one in methylene chloride (CH_2Cl_2; Figure 10). All four samples were taken from differently colored areas of the solid material shown in Figure 6. MALDI-TOF MS has been successfully applied in the analysis of transition-metal catalysts.[30] It stands out from other MS methods due to its unique ability to report on the molecular identity of intact metal complexes. An additional advantage is its capacity to identify complexes by their characteristic isotope patterns,[31] aiding in the discrimination among complexes with similar m/z ratios.

Figure 6. Mass of complex **11** after daylight exposure for about three weeks. Color changes from dark brown to khaki and partially green, as shown above

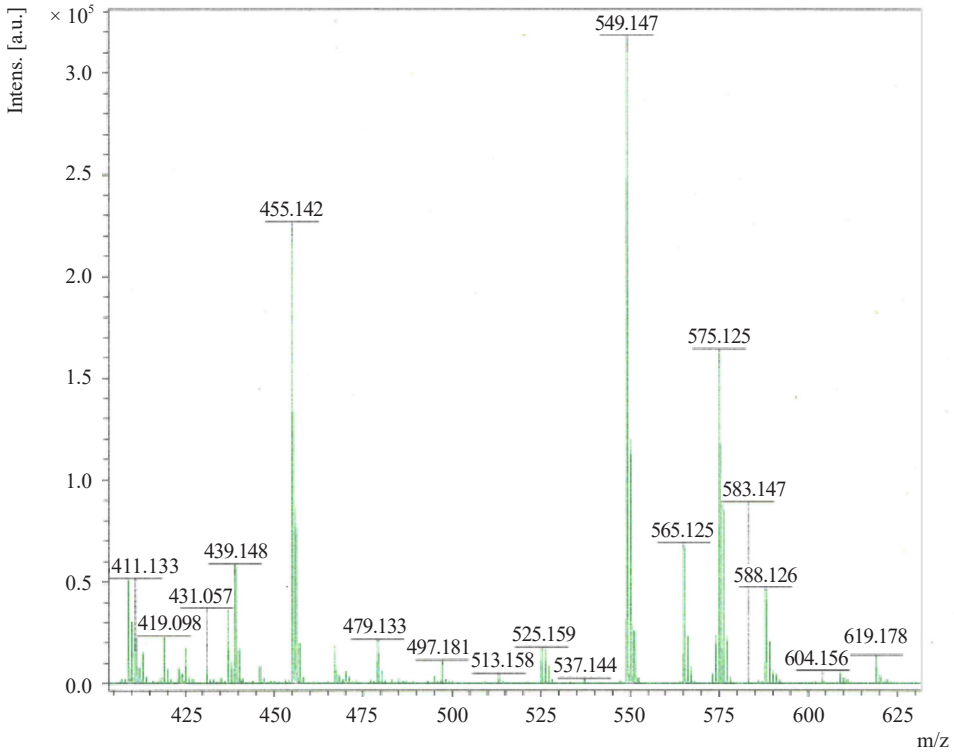

Figure 7. First MALDI-TOF spectrum of complex **11** in THF, after room-light exposure, as described in the text

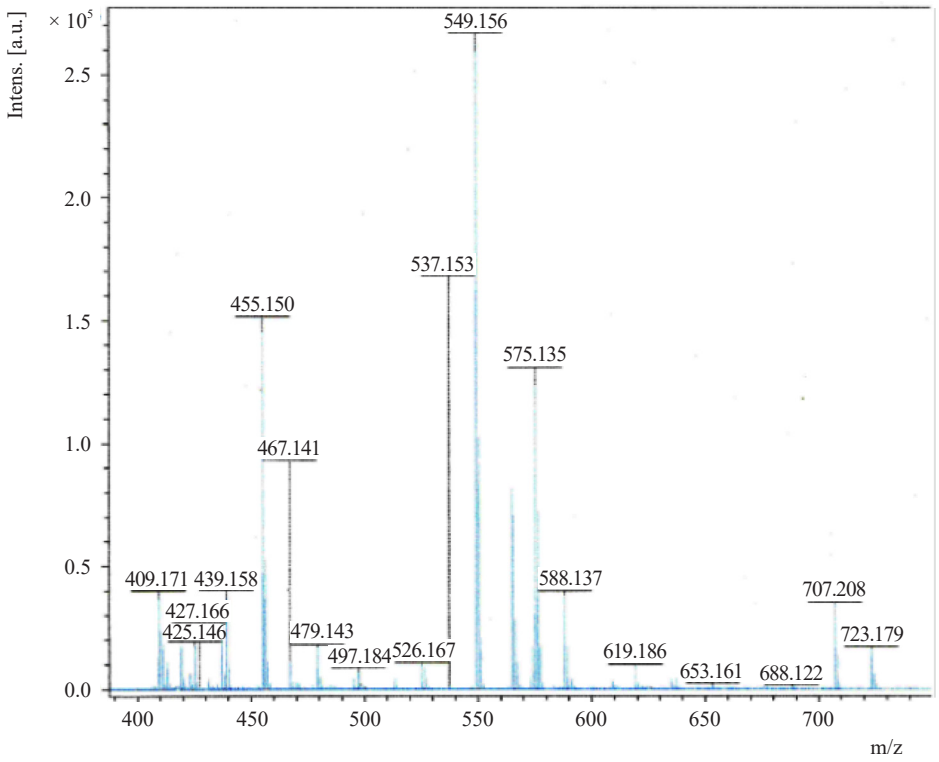

Figure 8. Second MALDI-TOF spectrum of complex **11** in THF, after room-light exposure

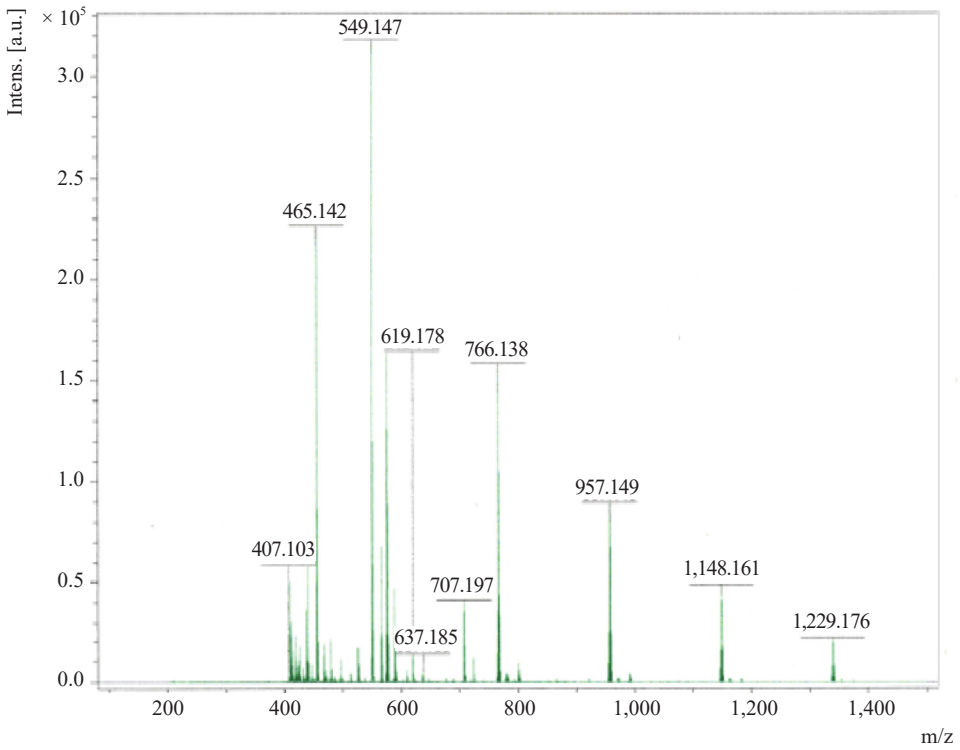

Figure 9. Third MALDI-TOF spectrum of complex **11** in THF, after room-light exposure. PI oligomers recorded

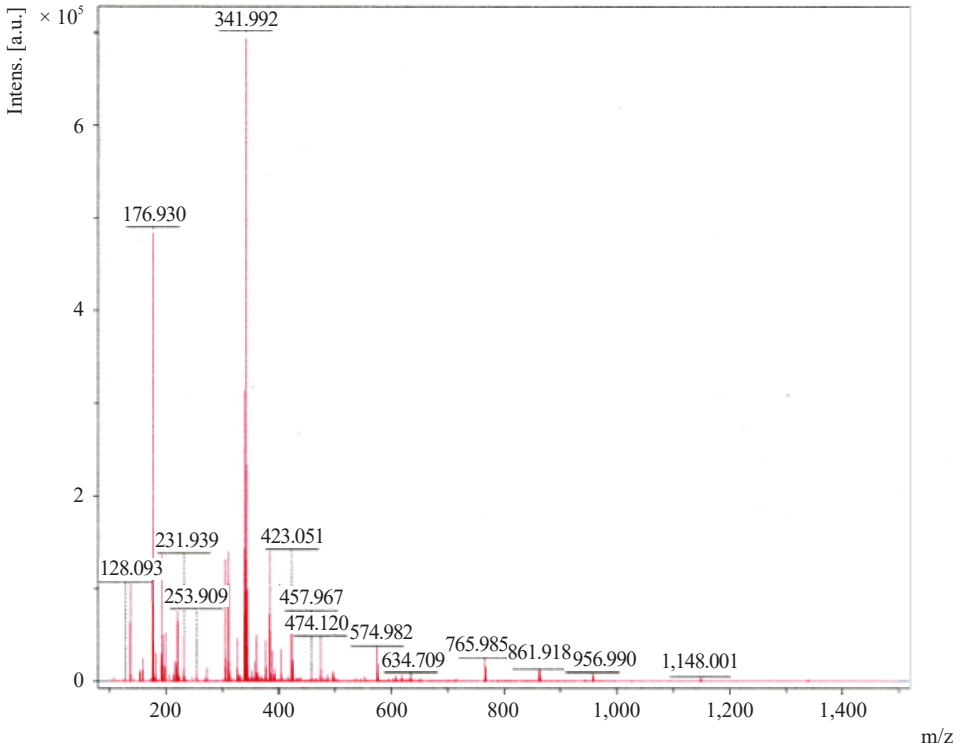

Figure 10. MALDI-TOF spectrum of complex **11** in CH_2Cl_2, after room-light exposure

The recorded MALDI-TOF data reveal important differences between the THF and CH_2Cl_2 solution data, likely due to the varying solubility of the components represented by the m/z data in each solvent. The MALDI-TOF m/z data for the THF samples (Figures 7-9) show close similarities among the strong peaks (mass/charge m/z 455, 549, 575), but also notable differences attributable to the uniquely differentiated transformations occurring in each specific spot/environment of the mass in Figure 6, from which each sample was taken. For example, there is a significant peak at m/z 537 in Figure 8, which is minor in Figure 7 and almost non-existent in Figure 9.

It is reassuring that the expected m/z number 575, representing complex **11**, appears in all MALDI-TOF spectra, although not as the strongest peak. For every peak assigned to a complex, we compared three key molecular data points: molecular weight (MW), m/z, and MS. For example, the data for complex **11** are as follows: the calculated molecular weight (MW) is 575.16, the expected m/z[32] (considering the isotope distribution of each element in the complex) is 574.00, and the experimentally recorded MS data points from MALDI-TOF are 575.125 in Figure 7 and 575.135 in Figure 8.

In addition to identifying the 575 peak (representing the originally prepared complex **11**), we expected to find the respective hydrolysis products in the MALDI-TOF data. The hydrolysis of complex **11** is expected to follow the analogous hydrolysis steps of $TiCl_4$ itself,[33] yielding complexes **11A**, **11B**, and **11C** (Figure 11) as active photocatalysts. However, to our initial disappointment, none of these hydrolysis products were recorded in the MALDI-TOF spectra.

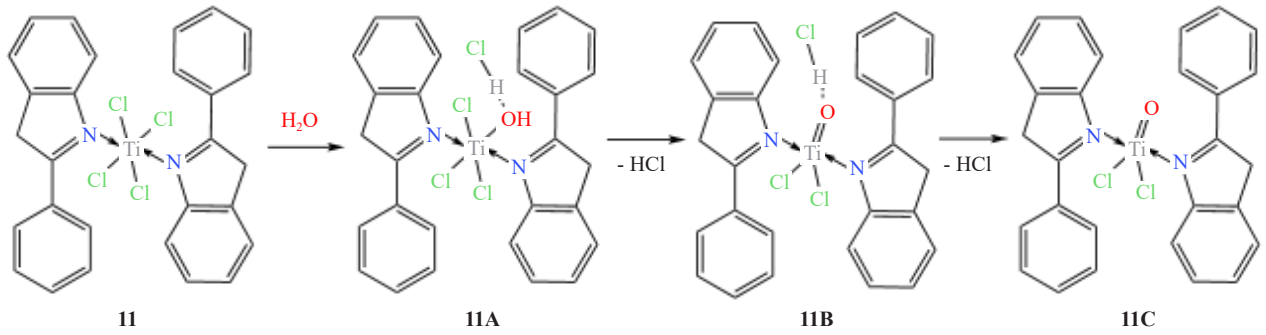

Figure 11. Expected hydrolysis products of complex **11**

Interestingly, the strongest peak in all three THF MALDI-TOF spectra is at 549 m/z, which corresponds well with a CO adduct of complex **11C** (MW 549.27, m/z 548.05, MS 549.147). The presence of the **11C**/CO complex led to the following fundamental realizations:

• The initially formed complex **11C** is now fully transformed and consumed by actively participating in the direct air capture (DAC) of CO_2. This is confirmed by the presence of an **11C**/CO_2 adduct (MW 565.21, m/z 564.05, MS 565.125) in Figure 7, and a second derivative adduct **11C**/CO_2/H_2O (MW 583.29, m/z 582.06, MS 583.147).

• The system can reduce CO_2 to CO, as indicated by the identification of both types of adducts.

• A Ti^{IV}/Ti^{III} redox system is unambiguously operating, as evidenced by numerous related intermediates (vide infra).

• Transfer hydrogenation of CO_2[34] to initially form CH_2O and CH_3OH, with their ultimate coupling into ethylene glycol, is indicated.

Furthermore, we have observed an event we now call structural sequencing. A cascade of complexes is being formed by the consecutive addition of "CO" and "CH_2" moieties to a growing linear carbon chain, which is part of an organotitanium complex. More on these unusual reaction types will be discussed below. Similarly, a Ti^{III} framework, 2PI·$TiCl_3$·$HOCH_2CH_2OH$, adds small molecules (H_2O, O_2, HCl) consecutively, forming a cascade of related adducts.

Guided by these realizations, the cascade additions of "CO" or "CH_2" to a carbon chain, the methodically organized sequence of organotitanium adducts, and some anticipated chemistry of the original complex **11** (i.e., hydrolysis), we propose the structural identification by MALDI-TOF spectra of all individual entities as shown in Figure 12. This includes a total of 25 new complexes and one PI trimer.

Besides relying on the close agreement of the experimental data (MS) with the actual and calculated values (MW,

m/z), each individual formula in Figure 12 has a high probability of existence based on structural similarities with known and reported organotitanium complexes. Arguments based on the expected reactivity of several individual complexes with CO_2 (formation of carbonates) and H_2O (hydrolysis products), along with the systematic cascade sequence of complexes **21**, **23**, **24**, and **25** through **29**, provide indirect evidence supporting the structural integrity of the complexes listed in Figure 12.

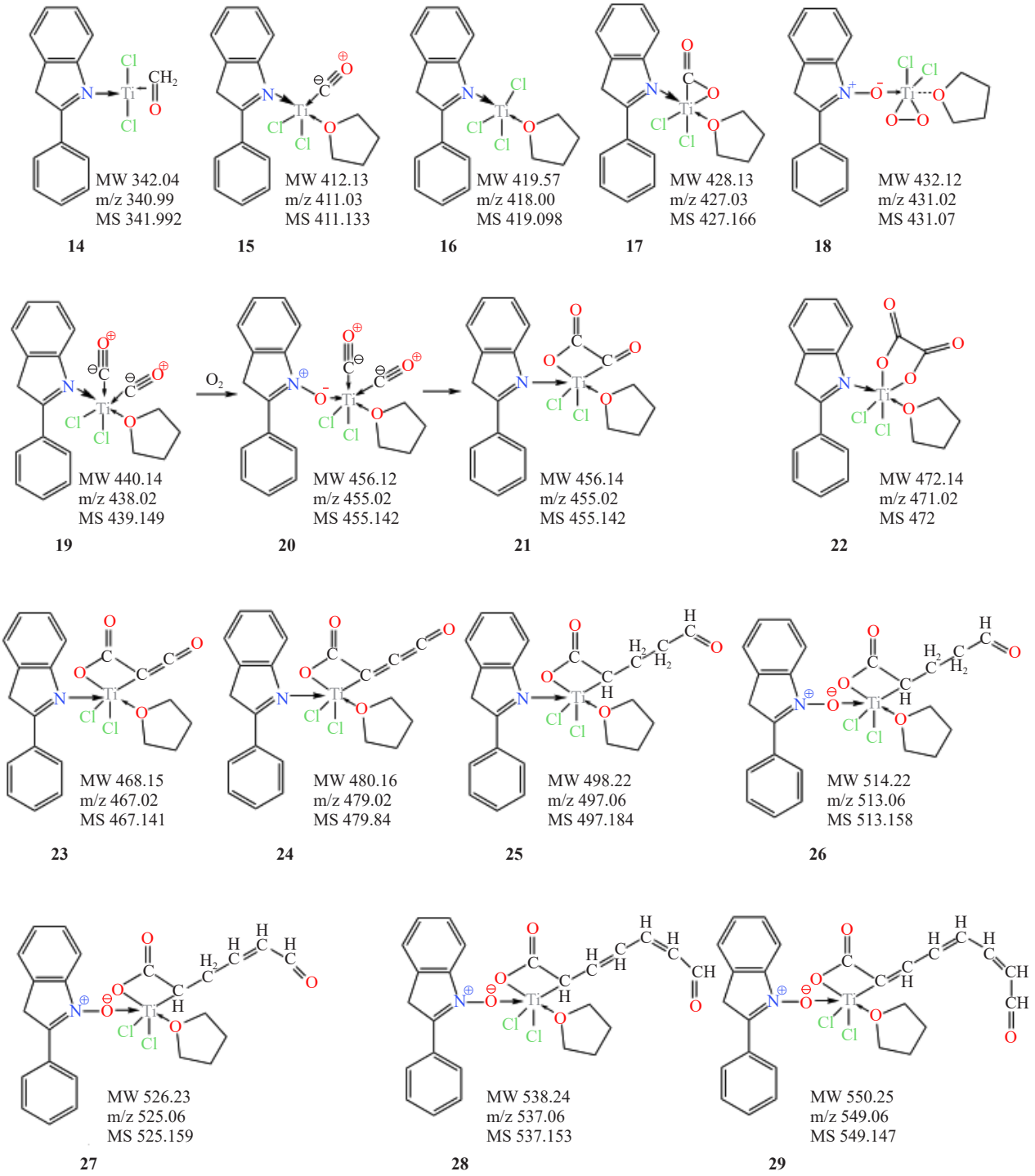

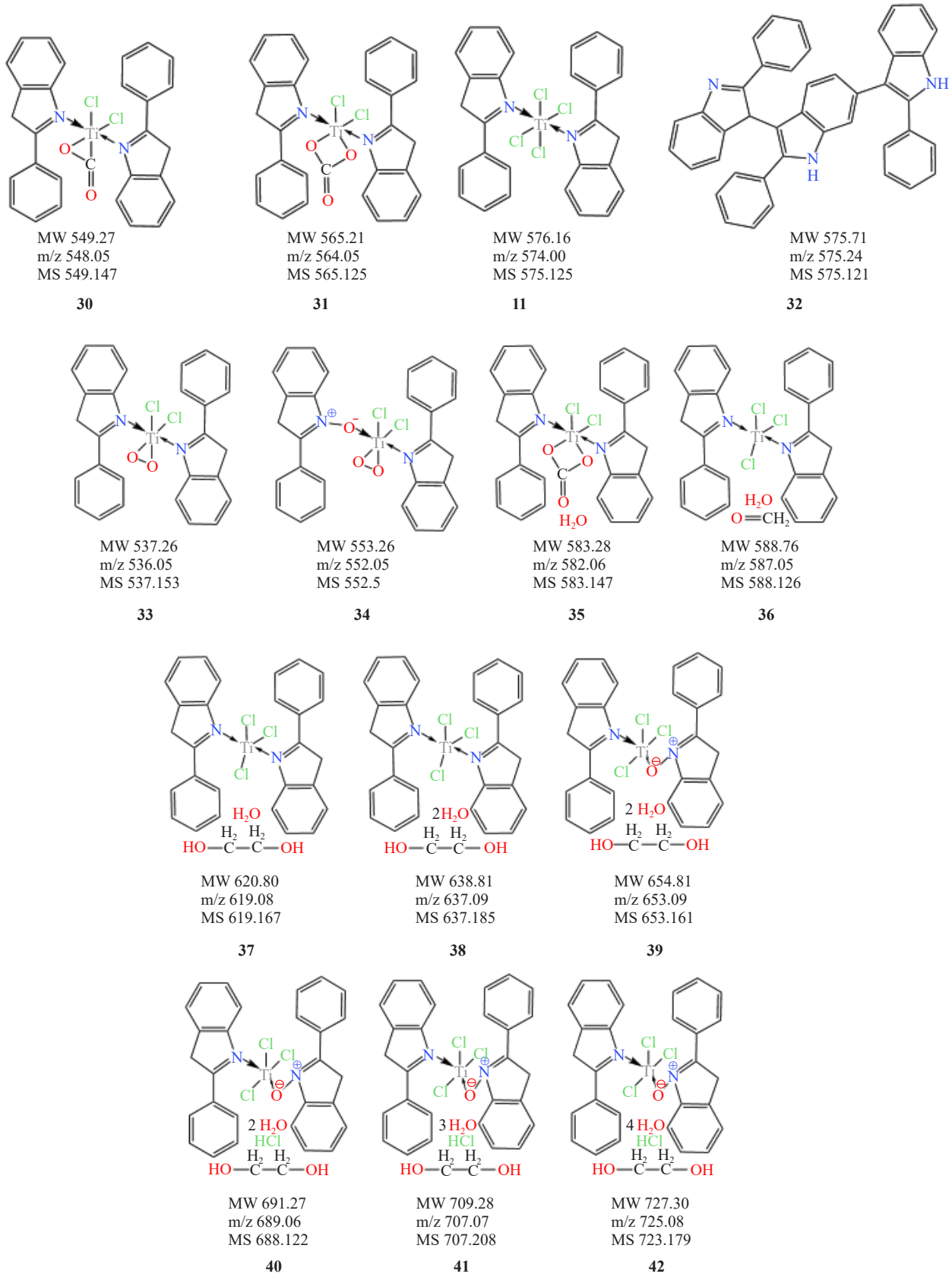

Figure 12. Organotitanium complexes identified from MALDI-TOF data of air- and visible light-exposed complex **11**

The presence of the THF ligand in several complexes originates from using THF as a solvent in the MALDI-TOF test. The complexes exhibit familiar properties and chemical behaviors, including ligand exchange (one PI replaced by THF in complexes **15** through **29**), reduction of carbonates[35] (**17**, **31**, **35**), redox reactions (**14**, **15**, **16**, **19**, **20**, **36-42**), CO coordination (**15**, **19**, **20**), peroxotitanium formation (**18**, **33**, **34**), oxalatotitanium formation (**22**), and oxidation/formation of 2-phenyl indole-N-oxide titanium (**18**, **20**, **26-29**, **40-42**). They also form adducts/coordination compounds with H_2O (**36-42**), formaldehyde (**14**), ethylene glycol[36] (produced by photocatalytic coupling of methanol and formaldehyde), H_2O (**37-39**)[36] and HCl (**40-42**).

The identification of these complexes provides strong evidence for several notable, new, and emerging processes, such as CO_2 capture by a Ti=O functionality (**31**, **35**), which mimics analogous CO_2 capturing by TiO_2.[37-38] Additional processes include the internal oxidative binding of two CO ligands (transforming complex **20** to **21**), reduction of titanium carbonate to titanium carboxylate (**31** to **30**), and a remarkable new type of linear carbon growth process represented by two structural sequences (**21**, **23**, **24**, and **25-29**). These sequences are precursors to long carbon-chain derivatives, representing a form of catalytic dehydration oligomerization between a ketone (**21**), a ketene (**23**, **24**), or an aldehyde (**25-29**) functional group, with system-produced formaldehyde as the building block.

Unexpectedly, products from the direct hydrolysis of complex **11** (see Figure 11) are absent from the list in Figure 12. As mentioned earlier, these complexes have been consumed by atmospheric CO_2 capturing, forming complexes **31** and **35**, and complex **30** after reduction.

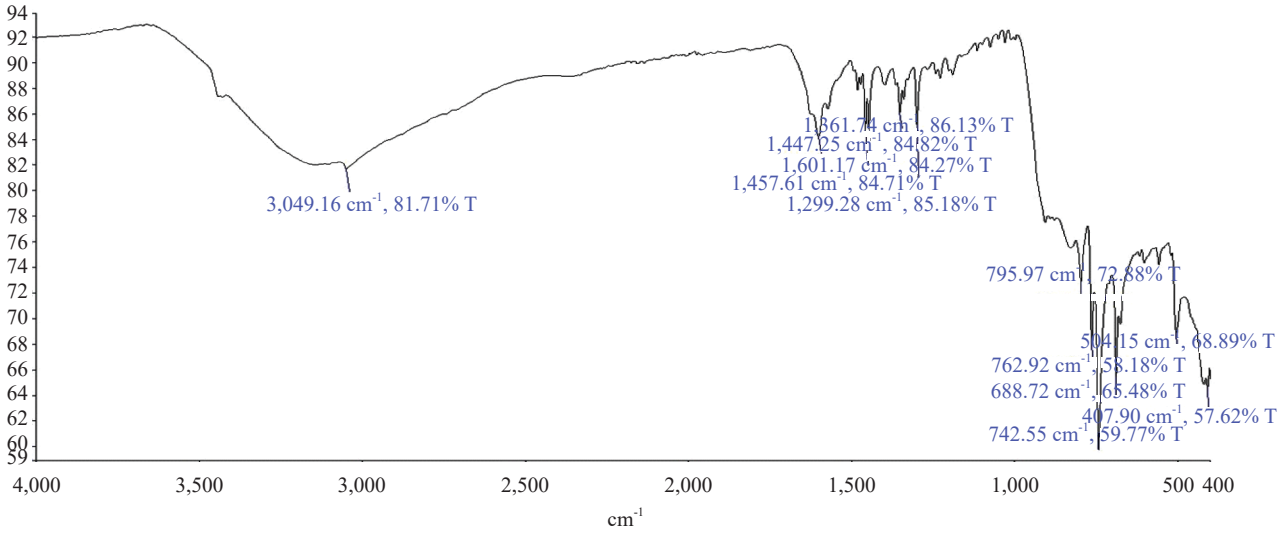

3,048.16 cm^{-1}	81.71% T	1,299.28 cm^{-1}	86.18% T	742.56 cm^{-1}	58.77% T
1,601.17	84.27	1,261.74	85.13	688.72	65.48
1,457.61	84.71	795.37	72.89	504.15	58.88
1,447.26	84.82	762.92	58.77	407.80	54.62

Figure 13. FTIR of the mixture of the 2:1 PI/$TiCl_4$ complex **11** after 3 weeks of visible light exposure. Peaks identified in the spectrum, with their corresponding transmittal values

The IR spectrum of the daylight- and air-exposed complex **11** was recorded (Figure 13) after approximately three weeks of exposure. Although extracting indisputable evidence from a single IR spectrum of a multi-component mixture (most of which are depicted in Figure 12) is challenging, functional groups can still be identified. Comparisons of IR absorptions were made using an established database.[39] The IR spectrum is predominantly characterized by PI absorption fingerprints in the ranges of 650-800 cm^{-1}, 1,300-1,500 cm^{-1}, and at 1,601 cm^{-1}. Additionally, the 408 cm^{-1}

peak is attributed to Ti-Cl vibration, the 839 cm^{-1} and the broad strong absorption at about 2,000-3,600 cm^{-1} are due to the presence of coordinated water and other alcoholic and/or carboxylic acid moieties. Notably, a 3,048 cm^{-1} peak is commonly assigned to C-H stretching of alkenes, and the 3,434/3,451 cm^{-1} absorptions are attributed to intermolecularly bonded alcohols. We suggest that the two weak absorptions at 1,021 and 1,047 cm^{-1} represent a fingerprint of coordinated ethylene glycol (see complexes **37-42**). The corresponding peaks in free ethylene glycol are at 1,042 and 1,087 cm^{-1}. The 1,631 cm^{-1} peak is assigned to an oxalate moiety (complex **22**) as well as the COOCO ligand of complex **21**. The carboxylate group of complex **30** is represented at 1,571 cm^{-1}. Several other important functionalities may be superimposed by PI absorptions, namely the carbonate (complexes **31**, **35**) at 1,457 cm^{-1}, the N-O group (complexes **18**, **20**, **26-29**, **39-42**) at 1,299 cm^{-1}, and Ti-O at 689 cm^{-1}. The peroxotitanium TiOO appears at 877 cm^{-1} (complexes **18**, **33**, **34**), and a peak at 895 cm^{-1} is possibly attributed to Ti=O.

The ^{1}H NMR spectrum of complex **11** in DMSO-d6 after exposure is shown in Figure 13. The absence of a chemical shift at 8.28 ppm, which represents the N-bound hydrogen, supports the notion that the coordinated PI exists in the indolenine form. Notably, a chemical shift at 5.77 ppm is assigned to the two protons on the 3-carbon of indolenine. Additionally, there are twenty major chemical shifts in the spectrum, compared to the eight corresponding chemical shifts assigned to the carbon-attached protons of PI.[39]

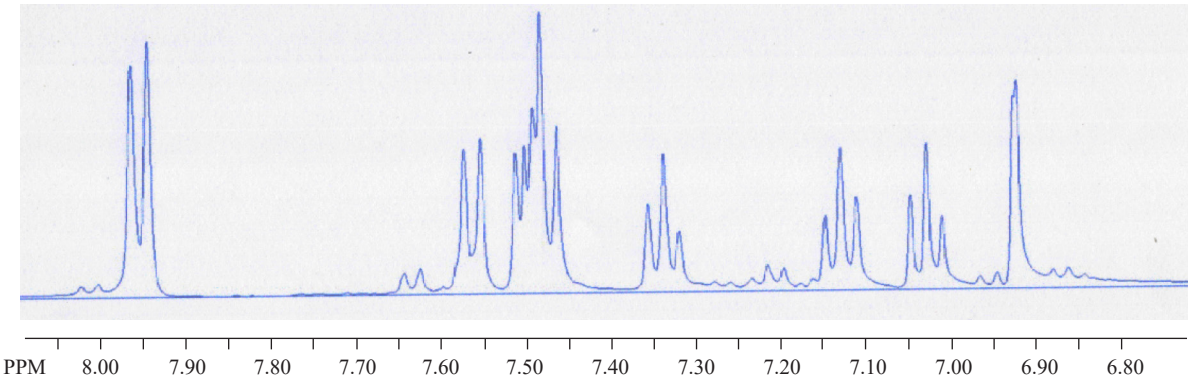

Figure 14. ^{1}H NMR of complex **11** after exposure to visible light and air

The multiplicity of chemical shifts attributed to the PI ligands indicates four or more types of coordinating modes:

a. Coordinated to Ti^{IV} through the indolenine N (complexes **14**, **17**, **19-25**, **30**, **31**, **33**, **36-42**).

b. Coordinated to Ti^{III} or Ti^{II} (complexes **14**, **15**, **16**, **36-42**).

c. Coordinated to Ti as the PI N-oxide (complexes **20**, **26-29**, **39-42**).

d. Forms PI oligomers (PI trimer **32**). A PI dimer is indicated by a weak signal at MS 384 (Figure 10), a tetramer at MS 766.136, a pentamer at 957.149, a hexamer at 1,148.161, and a heptamer at 1,339.176 (Figure 9).

Additionally, seven minor chemical shifts between 7.90 ppm and 7.15 ppm are assigned to hydrogen atoms attached to conjugated carbon bonds (complexes **27**, **28**, **29**).

Not shown in the spectrum of Figure 14 are chemical shifts at 11.65 ppm assigned to a carboxylic acid, at 3.47 ppm to -CH_2-O (complexes **37-42**), at 2.50 ppm for DMSO-d6-H_2O exchanged protons, and at 2.30 ppm assigned to RCOH (complexes **25-29**).

A ^{13}C NMR spectrum recorded at the same time as the ^{1}H NMR and the FTIR confirmed the presence of the PI chemical shifts, with minor positional variations, but without the δ-multiplicity seen in the analogous ^{1}H NMR.

The newly discovered interrelated organotitanium intermediates depicted in Figure 12 carry a wealth of information that may provide valuable guidance and innovative pathways in the energy field. For example, they elucidate the mechanism of the sunlight-catalytic splitting of water into hydrogen and oxygen by an identifiable molecular organotitanium system, while simultaneously capturing and reducing atmospheric CO_2 into C_1 compounds. These compounds are then transformed into feedstocks for creating new compounds with multiple C-C bonds, presenting a

novel route to artificial photosynthesis. Indeed, this is a groundbreaking and unexpected "living" photocatalytic system, comprising several intertwined and continuously operating individual processes, all supported by the inexhaustible resources of sunlight, air, and humidity.

We aim to carefully analyze each individual process and the interconnections among them to gain a comprehensive understanding of the synthetic modus operandi of the entire system. Our analysis indicates that the individual processes operating synergistically within the total photocatalytic system are as follows:

a. Hydrolysis of a Ti-Cl bond of the original complex **11** by air humidity, forming a Ti-OH and/or a transient, photoactive Ti=O bond, essentially creating a new PI complex of $TiOCl_2$ **11C** (Figure 11).

b. DAC of CO_2 under ambient conditions, resulting in the formation of cyclic carbonate organotitanium complexes.

c. Visible light photocatalytic reduction of Ti^{IV} to Ti^{III} and Ti^{II}, with the formation of peroxotitanium complexes through reaction with H_2O_2, which have enhanced photoabsorption in the visible range. This process also includes photocatalytic water oxidation, producing H_2 and H_2O_2, and N-oxidation of the PI ligand.

d. Reduction of captured CO_2 to CO, H_2CO, and CH_3OH using system-generated H_2. Photocatalytic coupling of H_2CO and CH_3OH to produce $HOCH_2CH_2OH$.

e. Formation of linear carbon chains, ranging from C_2 to C_7 and beyond, using system-generated formaldehyde as the building block.

f. Titanium ligand exchange, PI with donor molecules THF and formaldehyde, and the formation of adducts with H_2O, HCl, and $HOCH_2CH_2OH$, all formally participating in the visible light photocatalytic process.

g. 2-Phenyl indole catalytic oligomerization.

A detailed analysis of each process and their interactions will be provided to elucidate the overall system's operation.

2.1 *Hydrolysis of Ti-Cl bonds of complex 11 by air humidity: Formation of Ti-OH and/or a transient, photoactive Ti=O bond*

The key to activating our photocatalytic system, originating from complex **11** (and all other homologs illustrated in Figures 3-5), is the hydrolysis of a Ti-Cl bond by air humidity. This process forms Ti-OH and Ti=O functionalities, as suggested in Figure 11. Among the hydrolysis products, the highly photocatalytically active complex **11C** may also be directly accessible by the reaction of two equivalents of PI with one $TiOCl_2$, a compound available in pure solid form.

We propose that complex **11A**, the first hydrolysis product of the original complex **11** (Figure 11), or its HCl-free analog **43** (Figure 15), expels an OH radical under visible light irradiation, forming the Ti^{III} complex **44**. This fundamental reaction echoes the work of Beweries[15] and colleagues. The existence of multiple adducts of 44 in the photocatalytic sequence (**16**, **36-42**, Figure 12) supports this notion. Hydrogen-bonded HCl in **11C** may result in chlorine radical formation (·OH + HCl = H_2O + Cl·).[40] In fact, chlorine radical may be responsible for the observed para-chlorination of the phenyl group of PI. An OH radical plays a key role in H_2O splitting, as discussed below.

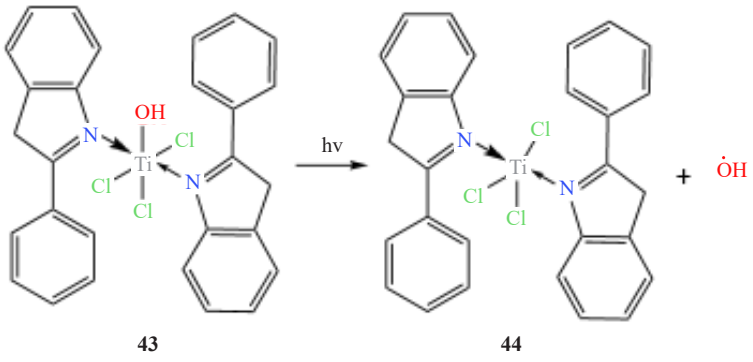

43 **44**

Figure 15. Visible light irradiation of the Ti^{IV} complex **43** produces hydroxyl radicals and reduces it to the Ti^{III} complex **44**

Furthermore, complex **11C** is expected to be highly hydrophilic, transforming into the dihydroxido complex **45** by air humidity (Figure 16). Visible light irradiation will again create hydroxyl radicals, and the transient Ti^{II} complex **46** will be readily available for DAC of CO_2, forming complex **30** (Figure 12), or coordinating system-generated small molecules CH_2O (**14**), CO (**15**, **19**, **20**), and even atmospheric O_2 (**18**, **33**, **34**).

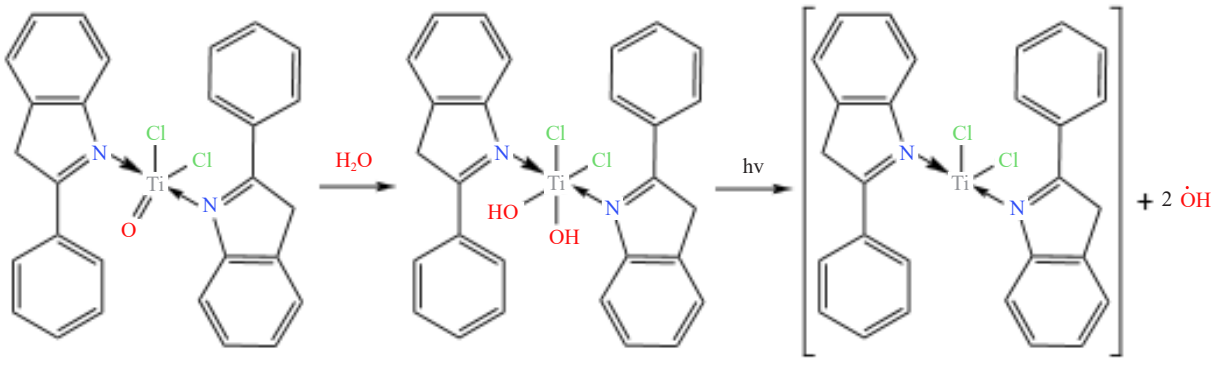

11C **45** **46**

Figure 16. Hydrolysis of complex **11C** to the dihydroxido complex **45**, irradiated by visible light to yield the transient Ti^{II} framework **46** and hydroxyl radicals

The existence of complex **46** raises the possibility of direct atmospheric nitrogen coordination, with implications for ammonia production, like previously reported Ti^{II} molecular nitrogen fixation under mild conditions.[41-42] However, this has not been observed under our experimental conditions. We believe competing reactions of **46** with atmospheric O_2 and CO_2 prevent N_2 coordination, which should be re-examined.

The Ti=O (Ti^{4+}-O^{2-}) bond of complex **11C** could be photo-excited as shown in Figure 17.

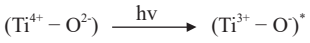

Figure 17. Photoexcitation of the Ti=O bond

This photo-excited functionality participates in the reduction of CO_2 to HCOOH and the oxidation of alcohols.[43]

The important photoactivated synergy of the PI ligand of complex **11C** with the central metal Ti and the core moiety Cl_2TiO, as well as a similar synergy in all other complexes of our photocatalytic ecosystem, is a form of Metal-to-Ligand Charge Transfer (MLCT).[44] We anticipate visible light photoionization of the PI ligand to form radical cation **47A**[24]/**47B** (Figure 18) and an electron, followed by Ti^{IV} reduction to Ti^{III}, creating the PI complex **48A** and a PI radical **48B**. Moreover, complex **48A** will have a propensity to photo-expel an OH radical (dimerizing to H_2O_2), forming the transient intermediate **48C**. This scheme is substantiated by the observed spontaneous radical oligomerization of PI in the system, and several reductions by the generated electrons, including the reduction of water to produce hydrogen.

2.2 *Direct atmospheric capturing of CO_2*

A remarkable and groundbreaking attribute of our visible light-induced catalytic system is the DAC of CO_2 under ambient temperature and pressure conditions. This system subsequently reduces CO_2 autonomously to useful organic materials, making it one of the few artificial chemical systems with such capabilities, like natural photosynthesis.

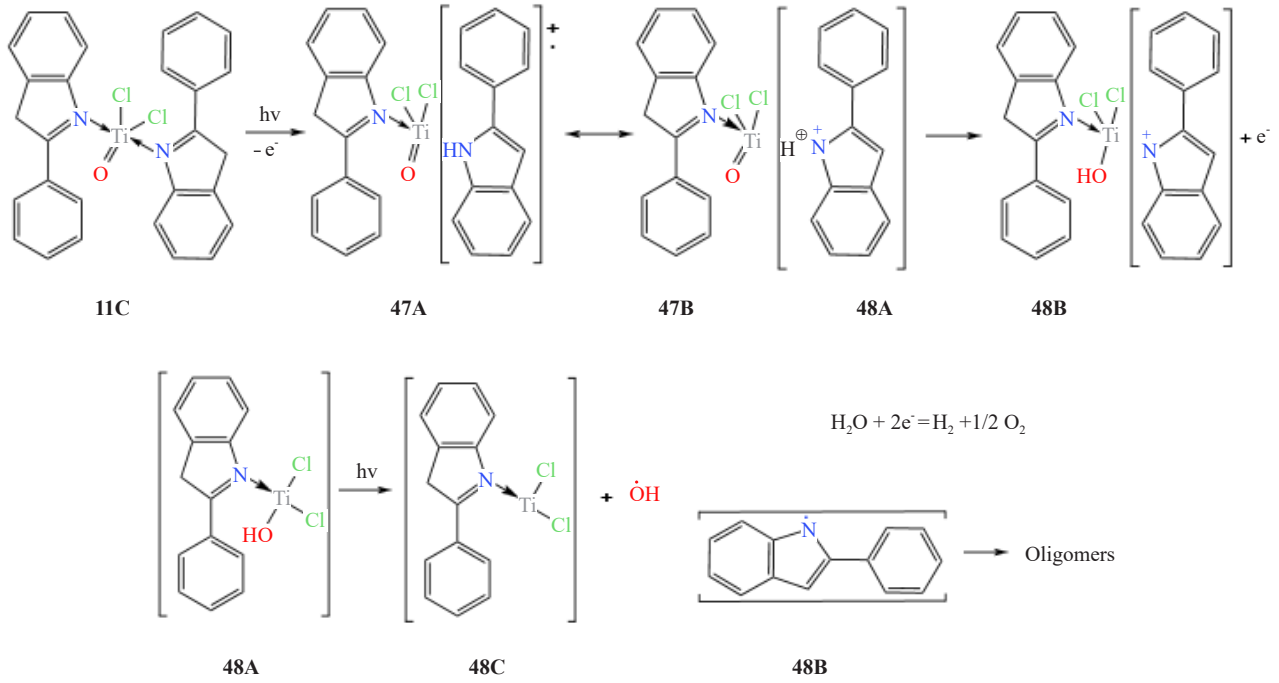

Figure 18. Photoionization of complex **11C** affecting the PI ligand, forming PI radical cation **47A**/**47B**, transforming to complex **48A**, the PI radical **48B**, and an electron. Second row: Photoionization of fragment **48A** to transient TiII intermediate **48C** and OH radicals; PI radical **48B** initiating PI oligomerization; and electrons splitting H_2O to hydrogen and oxygen

Solid evidence for DAC of CO_2 by our system includes complexes **17** and **30**, produced by the interaction of CO_2 with the transient Ti^{II} intermediate **46**, and complexes **31** and **35** from complex **11C**, facilitated by a photo-excited Ti=O bond, as shown in Figure 19.

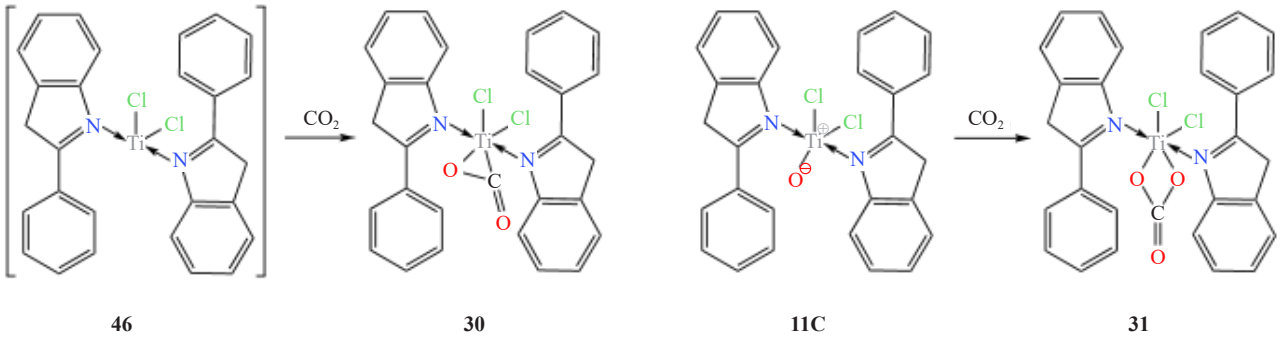

Figure 19. DAC of CO_2 by complexes **46** and **11C**

Complex **30** may also derive from complex **31** via its hydrolyzed form **35** (Figure 20). Under visible light excitation, complex **35** will expel a hydroxyl radical and rearrange to complex **35A**. The attack of an OH radical on the OH group of **35A** will produce H_2O_2 and the transient carbene **35B**, transforming it to complex **30**. This mechanism exemplifies a photocatalytic proton transfer from H_2O.

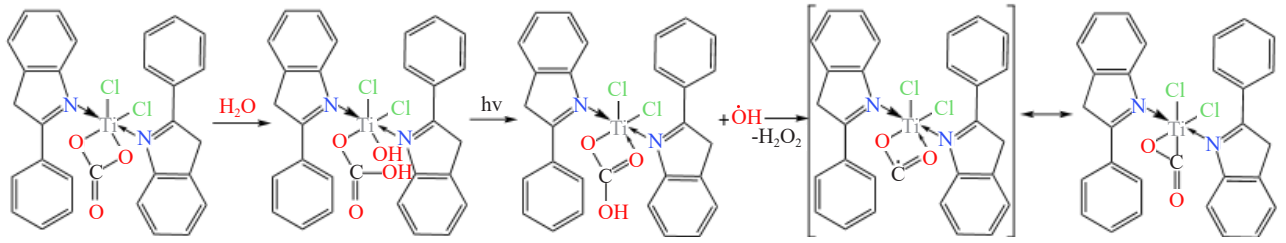

Figure 20. Photocatalytic reduction of complex **31** by hydrogen transfer from water, yielding complex **30**

While TiO_2 has been extensively used in the reaction[37] and photocatalytic reduction of CO_2,[38] there are no prior reports of a mononuclear titanium complex with a Ti=O functionality interacting with atmospheric CO_2 to form a carbonate group as in **31**. In contrast, other transition metal oxo complexes, such as those of Re and Mo, attract CO_2 to form MCO_3-type carbonates.[45] The complex $[(^tBu)(2,6\text{-diisopropylphenyl})N]_3Ti{=}O\ Li^+$ forms a bimetallic carbonate Li^+-O-(C=O)-O-TiR_3 with CO_2. Other types of CO_2 reactions with organotitanium compounds involve the insertion of CO_2 into Ti-C and Ti=NR bonds.

Carbonyl complexes **15** and **19** (Figure 12) can be considered derivatives of the Ti^{II} transient intermediate **46**, expected to exhibit chemical reactivity towards CO_2 like $Cp_2M(CO)_2$ (M = Ti, Zr),[46] promoting a Ti^{II}-mediated disproportionation of CO_2:

$$2CO_2 + 2e^- = CO_3^{2-} + CO$$

Disproportionation of captured CO_2 in our system aligns with the formation of carbonates **31** and **35** from **11C** (Figure 19), and $Ti(CO_2)$-type complexes **17** and **30** from **46**. However, the actual outcome with $Cp_2Ti(CO)_2 + {}^{13}CO_2$ is different, producing ^{13}CO and a dimeric dicarbonate Ti^{III} complex. The chemical behavior differences between $Cp_2Ti(CO)_2$ and complex **19** or **46** may be attributed to electronic and steric factors. $Cp_2Ti(CO)_2$, considered a "Cp_2Ti" carbene unit, is a stronger electron-pair donor to CO_2[47] than **46**, which has two electron-withdrawing chlorines attached to titanium. Additionally, the bulkier PI groups of **46** may prevent dimerization.

Further confirmation comes from the interaction of CO_2 with the bis(trimethylsilyl)-acetylene permethyltitanocene complex.[48] The production of $(Cp_2Ti(CO)_2$ and $(Cp_2Ti)_2CO_3$ verifies the disproportionation of CO_2 as a common mechanism in the presence of a formally Ti^{II} moiety. The bulkier and stronger electron donor Cp_2*Ti, compared with Cp_2Ti, promotes the formation of a Ti^{III} dimeric carbonate $(Cp_2Ti)_2CO_3$, an intermediate between the monomeric **31** (like carbonates of Re, Mo) and the dimeric carbonate derived from $Cp_2Ti(CO)_2$.[46] The monomeric $Ti(CO_2)$ complexes **17** and **30** are regarded as OTiCO insertion products,[49] previously identified in matrix isolation studies, though not commonly indicated in chemical literature.

The monocarbonyl complex **15** and the analogous dicarbonyl **19** may originate from complex **46** (Figure 16) or **48C** (Figure 18) and CO, resulting from disproportionated CO_2. An apparent catalytic oxidation (by H_2O_2 from the dimerization of OH radicals) of the PI ligand to the N-oxide (complex **20**) will result in a Ti-mediated oxidative C-C coupling of the two carbonyls to create complex **21**. This reaction, though unprecedented, appears plausible based on the sequence of identified complexes **19**, **20**, and **21**. Alternatively, complex **21** could be the product of CO insertion into the Ti-C bond of **17**. Further oxidation of **21** will yield the half-oxalate complex **22**, with oxalate being an established anion for Ti.

Complex **21** constitutes the basic material/catalyst for a new type of condensation oligomerization, producing oxygenated linear carbon chain materials. The mechanism of this unexpected product formation will be discussed in the following sections.

2.3 *Visible light photocatalytic reduction of Ti^{IV} to Ti^{III} and Ti^{II}: Formation of peroxotitanium complexes with enhanced photoabsorption in the visible range*

Starting with the original Ti^{IV} complex **11** (Figure 12), our system autonomously transforms under visible light irradiation, producing a plethora of interrelated new organotitanium complexes and intermediates in all three titanium oxidation states: Ti^{IV}, Ti^{III}, and Ti^{II}. The visible light photoreduction mechanism can follow different pathways, reducing Ti^{IV} to Ti^{III} (Figure 15), Ti^{IV} to Ti^{II} (Figure 16), or stepwise from Ti^{IV} to Ti^{III} and then to Ti^{II} via the transient Ti^{II} complex **48C** (Figure 18). These reductions occur with the synchronous formation of hydroxyl radicals (Figures 15, 16) and PI radicals (Figure 16), which initiate their own coupling (oligomerization) cycles within the active catalytic system. The hydroxyl radicals dimerize to form hydrogen peroxide, are responsible for the N-oxidation of PI ligands in complexes **20**, **26-29**, **34**, **39-41**, and the peroxidation of **11C** to yield complexes **18**, **33**, and **34** (Figure 21) and other oxidative attacks, as shown in Figure 20.

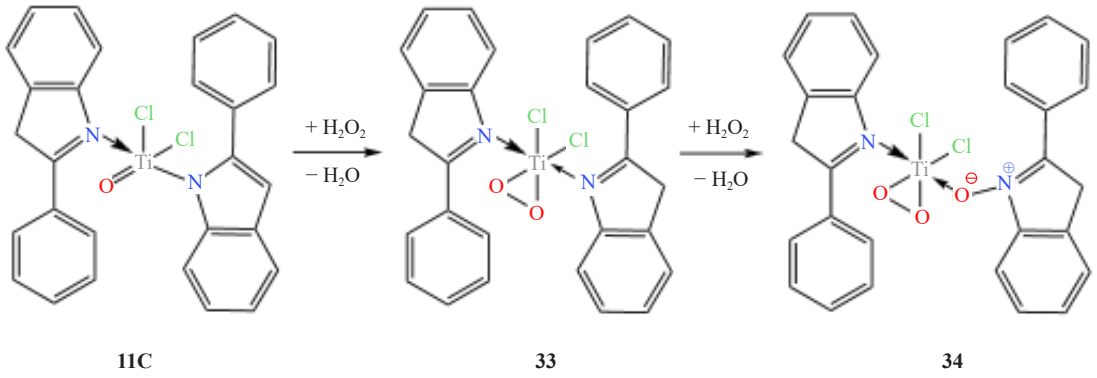

Figure 21. Peroxidation of complex **11C** with H_2O_2 to form the peroxotitanium complex **33** and the N-oxide PI complex **34**

Several studies[11,50] suggest that Ti-O-O coordination bonds effectively enhance visible light-induced photoactivity by shifting the photoabsorption region to the visible range of 400-800 nm. We propose that peroxotitanium complexes **18**, **33**, and **34**, or in general, complexes of the "Cl_2Ti-O-O" moiety coordinated with photocatalytically active ligands, are powerful photocatalysts for water splitting to H_2 and H_2O_2. The proposed water-splitting photocatalytic cycle involving complex **33** is depicted in Figure 22. Essentially, the coordinated water molecule **49** is photo-ionized by the PI ligand, forming a hydroxyl radical, a proton, and a hydrated electron **50**, as described by the equation:

$$H_2O \rightarrow \cdot OH + H^+ + e^-(\text{hydrated})$$

The hydroxyl radicals dimerize to form H_2O_2, while protons and electrons combine to form hydrogen gas.

Water forms a stronger hydrogen bond with the N-oxide of complex **34** compared to complex **33**, making the photocatalytic cycle even more efficient.

The concentration and action of complex **33** are "topical," meaning they are not homogeneous throughout the entire mass shown in Figure 6. For example, the MALDI-TOF peak at 537.144 in Figure 7, representing complex **33**, is minor, whereas the same peak in Figure 8, (a MALDI-TOF from a sample taken from a different area of the mass) is very prominent.

Complexes **33**, **34**, and related group 4 metal peroxo derivatives could be synthesized independently, for example, by reacting complex **11** with aqueous H_2O_2. These complexes can be further investigated as custom catalysts for visible light splitting of water to produce hydrogen.

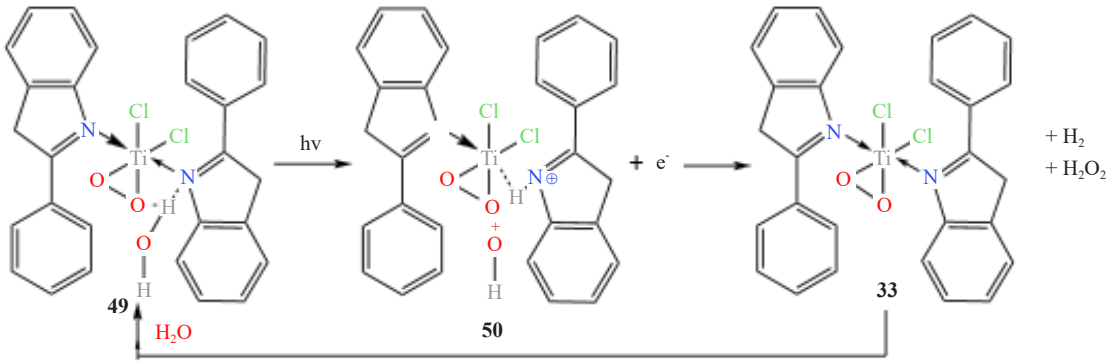

Figure 22. Proposed visible light photocatalytic cycle for water splitting to H_2 and H_2O_2 catalyzed by the peroxotitanium complex **33**

2.4 *Reduction of captured CO_2 to CO, H_2CO, and CH_3OH with hydrogen transfer from water or system-generated H_2*

Hydrogen produced by water splitting (Figures 18 and 22) will likely be consumed by various hydrogenation reactions within the system.

2.4.1 *Hydrogen reduction of $TiCl_4$-complex*

The hydrogen reduces the original $TiCl_4$-complex (**11**) to $TiCl_3$-complexes (**16**, **36**-**42**).

2.4.2 *Transformation of carbonyl complex*

The carbonyl complex (**15**) is transformed into the formaldehyde complex (**14**).

2.4.3 *Hydrogenation of cyclic carbonates*

Cyclic carbonates[35] **31**, (Figure 23) and **35** undergo hydrogenation to yield formaldehyde (**31B**) and methanol (**31C**), which then couple catalytically[36] to produce ethylene glycol, incorporated in complexes **37**-**42**. This process involves a catalytic sub-cycle through these steps, with the core complex in **31C** regeneration of CO_2.

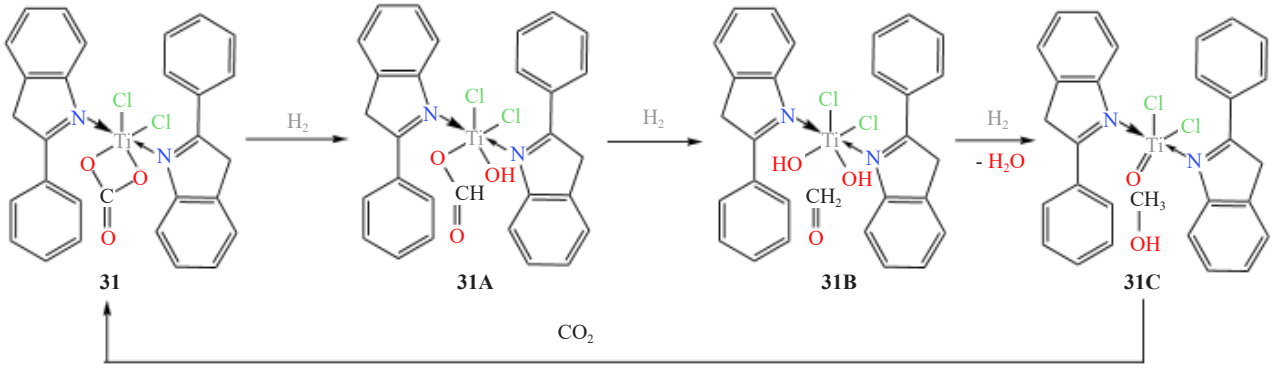

Figure 23. Reduction of the cyclic carbonate complex **31** to yield formaldehyde and methanol, with the catalytic cycle regenerating **31** using atmospheric CO_2

Complex **31** can be applied separately as a homogeneous or heterogeneous catalyst for the low-temperature and pressure hydrogenation of CO_2 with hydrogen.

2.4.4 *Hydrogenation of unsaturated organic derivatives*

An unsaturated organic derivative, complex **24**, is hydrogenated to form complex **25**.

No attempt has been made to detect any system-generated free hydrogen. However, we believe free hydrogen generation is possible, for example, through the catalytic cycle shown in Figure 22 using visible light in an atmosphere with controlled moisture. Complex **33** (Figure 22), being a fully saturated Ti^{IV} compound, does not interact with CO_2, unlike complexes **46** and **11C** (Figure 19).

As shown in Figure 20, hydrogenation can also be accomplished by hydrogen transfer from water. Similarly, complex **30** (Figure 24) may undergo hydrolysis to form **30A**, which under visible light irradiation expels a hydroxy radical and forms intermediate **30B**. Both species interact to ultimately produce the formaldehyde complex **30C**.

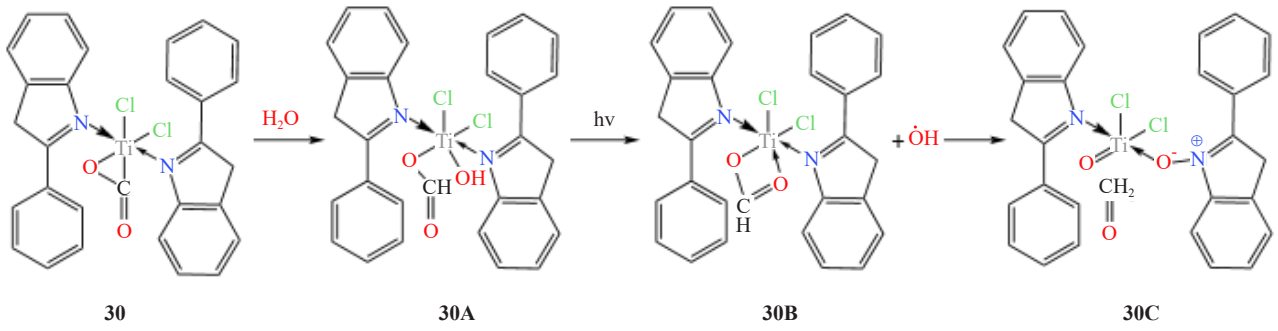

Figure 24. Photocatalytic reduction of complex **30** by hydrogen transfer from H_2O to form complex **30C**, with formaldehyde coordination

2.5 *Formation of linear carbon chains*

The photocatalytic system utilizes formaldehyde, a product of DAC CO_2 reduction, as a building block to produce long (C_2 to C_7 and beyond) linear carbon chains with oxygenated alpha-omega functionalities. We have identified complex **21**, an unusual titanium α-ketocarboxylate complex, as the catalyst for this novel reaction type-a dehydration synthesis between formaldehyde and the keto group of complex **21**, leading to the ketene functionality of complex **23**. An identical one-carbon growth of ketene continues with the formation of complex **24** (Figure 25), which is then hydrogenated to convert the ketene chain into aldehyde **25**.

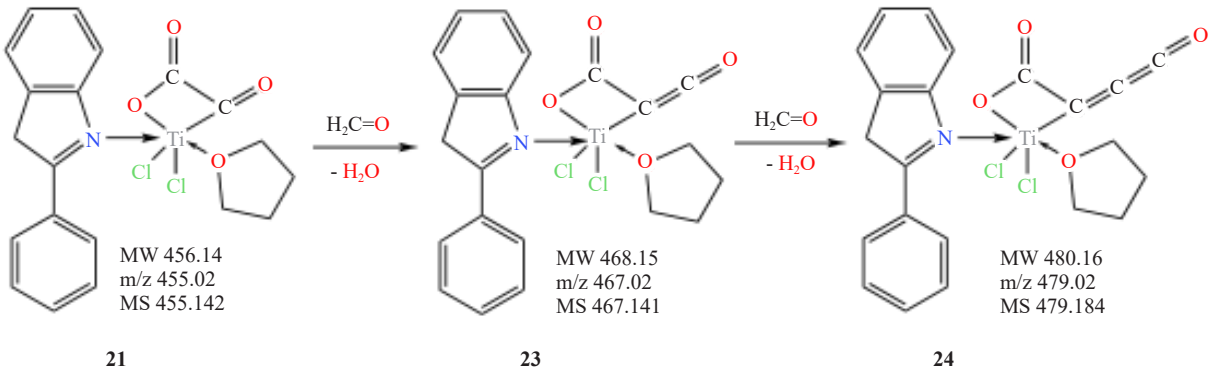

Figure 25. Photocatalytic carbon chain growth utilizing system-generated formaldehyde

We propose two possible pathways for the formation of photocatalyst **21**:

• By a CO insertion into the Ti-C bond of complex **17**.

• By an internal oxidative coupling of complex **20**.[51]

Titanium PI/THF dichloro dicarbonyl complex **19** plays a groundbreaking role in the reaction sequence leading up to complex **21**. Oxidative coupling is enacted by the N-oxidized PI ligand of the intermediate complex **20** (Figure 12).

The question arose whether the ketene and cumulene type complexes **23** and **24** are stable enough to even exist. The stability of ketenes is influenced by electron-withdrawing groups (EWG) within the molecule. For example, ketene-pyridine[52] is a stable molecule due to the electron-withdrawing properties of the nitrogen in pyridine. Similarly, the strongly electron-withdrawing carboxylate group in complexes **23** and **24** will stabilize these molecules. Additionally, the "$TiCl_2$" moiety at the Ti^{VI} oxidation state is highly electron deficient. The presence of chlorine atoms, being electronegative, further enhances the electron-withdrawing nature of the complex, contributing to its stability.

Another N-oxidation of the PI ligand in complex **25** generates complex **26**, which initiates a new sequence, culminating with complex **29**. This time, the chain growth occurs via an aldehyde function reacting with formaldehyde, based again on dehydration, generating three new consecutive complexes **27**, **28**, and **29** (Figure 12).

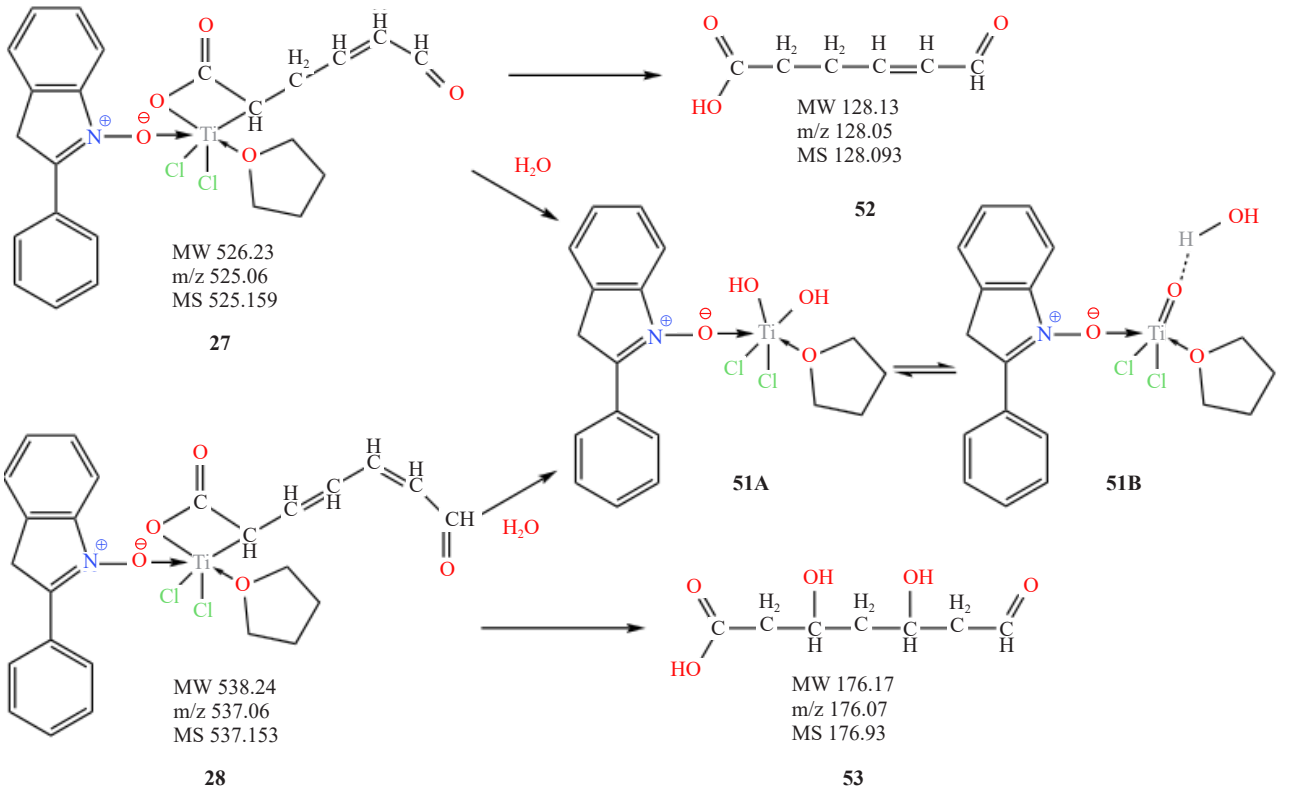

Figure 26. Oxygenated linear organic chains **52** and **53** are produced by the photocatalytic system after hydrolysis of complexes **27** and **28**, respectively. Creation of new photocatalysts **51A**/**51B**

The unprecedented carbon growth reactions manifested by complexes **21**, **23**, **24** (Figure 24), and **25** through **29** are responsible for the creation of the linear carbon chains, featuring alpha-omega (and other) oxygenated functionalities. We have identified two such products originating from the hydrolysis and/or double bond hydration of complexes **27** (product **52**) and **28** (product **53**) (Figure 26), recorded by the MALDI-TOF spectrum (Figure 10). The common titanium species from the hydrolysis is complex **51A**/**51B**, expected to be a powerful photocatalyst as well.

To our knowledge, it is the first-time products like **52** and **53** have been generated by any known artificial photocatalytic system. Given more time, the prospects for further chain growth are open. The resemblance of

these products to sugars is striking: six and seven carbon chains, an aldehyde, with hydroxyl and carboxylic acid functionalities.

Currently, long chain hydrocarbon products directly from CO_2 are obtained only by electrochemical conversion.[53] Cyanobacteria and algae are commonly used, as they naturally convert CO_2 into biomass, which can be processed into long-chain hydrocarbons. TiO_2 is a widely studied photocatalyst, though it primarily produces short-chain hydrocarbons. Now, for the first time, we obtained long-chain hydrocarbon products through mononuclear organotitanium complexes.

2.6 *Titanium ligand exchange and PI with donor molecules: THF, formaldehyde, and adducts in photocatalysis*

The mixed PI/THF titanium chloride coordination compounds (Complexes **15** through **29**, Figure 12) result from dissolving the bis-PI titanium complexes in THF for the MALDI-TOF test. These mixed-donor complexes demonstrate a facile exchange of at least one PI ligand from the original bis-PI complexes with other donor molecules like THF or system-generated formaldehyde, as seen in complex **14**.

The exchange of a single PI ligand with another donor molecule, rather than both PI ligands, might imply a steric effect (replacing a bulky ligand with a smaller one) or suggest that one PI ligand has a more labile Ti-N π-bond than the other. For example, complex **17** (mixed PI/THF ligands) and complex **30** (PI/PI) both appear in the roster. This facile ligand exchange may significantly impact the overall efficiency and operation of our photocatalytic system.

The prominent peak in the MALDI-TOF spectrum at m/z 341.992 is assigned to the PI·$TiCl_2$·H_2CO complex **14**, while the peak at m/z 413 may be attributed to a homolog with coordinated THF. Another notable peak at m/z 340 corresponds to PI·$TiCl_2$·CO, a homolog of complex **15** minus the coordinated THF. These findings support the idea that THF coordination in complexes **15** through **29** might be an artifact of using THF as a solvent during the MALDI-TOF test, indicating that these complexes may exist free of THF coordination. Systemic complexes with open and available coordination sites on titanium will facilitate the coordination of system-generated donor molecules like CO, CO_2, H_2CO, CH_3OH, and HCl, allowing them to actively participate in the AP process.

The $(PI)_2TiCl_3$ framework appears in three forms (**36-38**) among the titanium complexes in Figure 12, while complexes **39-42** (PI·PIO·$TiCl_3$) form adducts with combinations of H_2O, H_2CO, $HOCH_2CH_2OH$, and HCl. Complex **16** (PI·THF·$TiCl_3$) is also present. These Ti^{III} complexes are actively involved in the visible light-energized multiple redox operations of the photocatalytic system. For instance, we propose the visible light transformation of the TiIII complex **36** to the formally Ti^{II} complex **14** (Figure 27). Although the PI·HCl salt **54** is not represented in MALDI-TOF Figure 10, its pyrrole-hydrogenated analog is traced at MS 231.939.

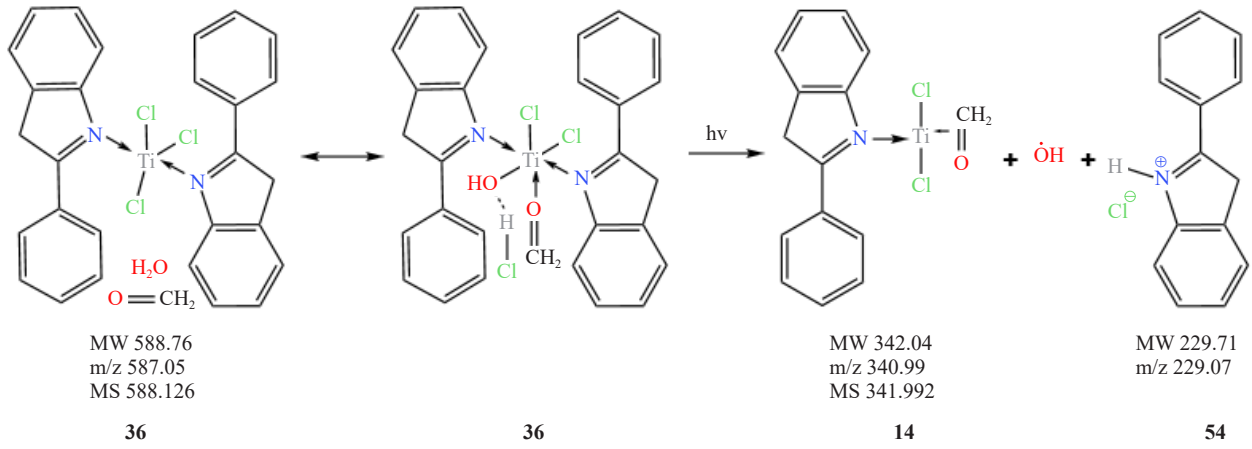

Figure 27. Visible light photocatalytic reduction of the Ti^{III} complex **36** to the formally Ti^{II} complex **14**

The formal presence of H_2O in complexes **36-40** indicates their participation in the photocatalytic process by generating hydroxyl radicals, like the mechanism depicted in Figure 27.

Methanol, an expected product of CO_2, CO, or H_2CO reduction within our system, could not be detected in a directly identifiable form, such as a Ti-OCH_3 moiety. However, closer examination of complexes **37-42** reveals a calculated molecular entity of "H_2CO+CH_3OH" present as an adduct in all of them. This entity is ethylene glycol ($HOCH_2CH_2OH$), produced by coupling formaldehyde and methanol through an efficient [Ti=O] photocatalyst, as described earlier.[36]

2.7 *2-Phenyl indole (PI) catalytic oligomerization*

As mentioned earlier (Figure 18), the oligomerization of photoionization-induced PI radical **48B** occurs simultaneously with other system operations, as evidenced by the cascade sequence of 2× up to 7× PI oligomers, registered in all MALDI-TOF tests. Figure 28 depicts oligomers 2× through 4× with their calculated m/z values and graphic representation of their corresponding estimated isotope distribution. The actual m/z values from all MALDI-TOF runs compared to the calculated values are within 0.4 m/z units or less, representing an excellent match. The appearance of all consecutive oligomers in MALDI-TOF in diminishing concentration indicates that they coexist and most likely are active participants in the oligomerization process. Supporting evidence is provided by the calculated isotope distribution,[32] which closely matches the recorded fingerprints of MALDI-TOF.

Like the coupling of 2-methylindole,[54] the oligomerization of PI is proposed to occur at the 3 and 6 linkage sites of the monomer, as shown in Figure 28. An indole oligomer may be electroconductive and fluorescent. It is not yet known whether these two properties will affect the photocatalytic process of the system.

The PI oligomerization deprives the complexes (Figure 12) of at least one of the two PI ligands on titanium. Currently, it is unclear whether the oligomerization is detrimental to the prolonged operation of the system or if the oligomers play any role in the overall effectiveness of the photocatalytic system. These important questions should be further investigated.

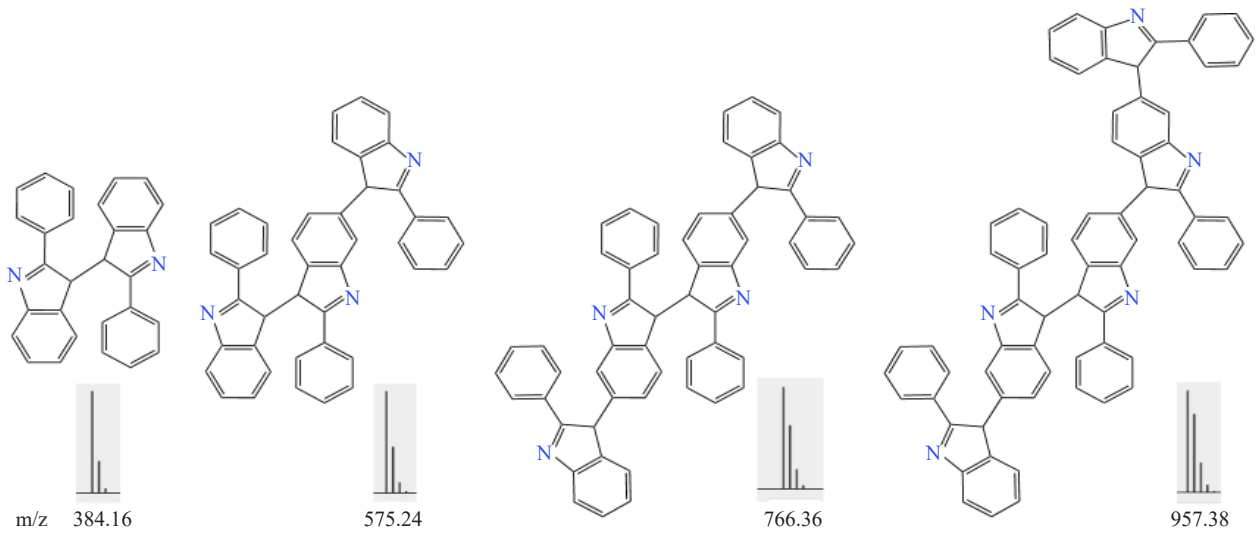

Figure 28. PI oligomers 2×, 3×, 4×, and 5× are produced by the visible light photocatalytic system. Calculated MALDI-TOF m/z with isotope distribution for each oligomer

3. Conclusion and outlook

The AP system described in this paper originates from a single source comprising easily accessible organotitanium complexes. These complexes transform through atmospheric humidity, visible light, and the direct air capture (DAC) of

CO_2 into a self-organized assembly of several intertwined, semi-autonomous, newly discovered processes.

Numerous interrelated organotitanium complexes, constituting the backbone of these processes, have been identified through MALDI-TOF MS spectra. These complexes operate in tandem to produce unexpected organic materials, including an autonomous DAC of CO_2, the formation of carbonated titanium complexes, their reduction by hydrogen transfer from H_2O, and/or the splitting of H_2O into hydrogen and H_2O_2/O_2. Energized by visible light, the system initially produces versatile C_1 organics, followed by the construction of long-chain (C_2 to C_7 and beyond) oxygenated hydrocarbons. No other known AP system has produced such higher molecular weight organics. If this process can be conducted cost-effectively and at scale, it would represent the most efficient single-shot method of storing sunlight in the form of versatile fuels known to humankind.[55]

Significant progress has been made globally on the two crucial steps of AP:

• Developing catalysts that use solar energy to split water into oxygen and hydrogen.

• Discovering catalysts that can convert hydrogen and carbon dioxide into energy-dense fuel.

The most important task is to combine these two steps within a single operating system,[55] in an affordable and scalable way, using cheap and earth-abundant catalytic materials. We believe our system fulfills this prerequisite, combining both conditions in a self-propelled, automatic, and efficient manner. It is based on titanium, the ninth most abundant element and the second most abundant transition metal in the Earth's crust.

Commercially applied DAC of CO_2 is energy-intensive, requiring chemical absorbents, ionic liquids, etc., with subsequent storage necessary for prior utilization. Our system captures CO_2 spontaneously and directly from the atmosphere under ambient temperature and pressure for immediate, on-the-spot utilization, bypassing any need for storage. This fact is most unusual and remarkable, and it appears our man-made system is the only one developed so far that fully mimics natural photosynthesis in this respect.

The isolation and characterization of a string of organotitanium intermediates, harmoniously interacting with each other in creating new products, provides solid evidence and insight into how the system operates. This know-how is indispensable for monitoring, improving intrinsic efficiency, and stabilizing the system for prolonged scale-up operation. Independent processes like H_2O splitting for the exclusive production of hydrogen are possible by utilizing the approach outlined in Figure 22. In this respect, the advantage of catalytic complex **33** is that it is inert toward CO_2.

The unequivocal identification of PI oligomers created by the system, as well as certain other complexes (e.g., **11**), by MALDI-TOF tests lends support to the identity of all other units in our active photocatalytic system. Identity is further strengthened by other factors, such as material sequences discussed earlier, similarities with existing chemical structures/complexes, and supporting information from IR and NMR data.

The system will need further refinement and quantitative evaluation. The conditions for optimum operation must be accurately defined. At this stage, we regard it as a promising new beginning with potential practical applications in scale-up operations.

An expanded investigation should cover the following topics.

3.1 *The role and efficiency of titanium compared with alternative central metal atoms*

Other group 4 elements (Zr, Hf) and even V are good candidates to replace Ti in the photocatalytic system. Especially Zr presents itself as the best alternative replacement for Ti, since the two metals share similar chemistry, forming identical PI complexes.[22] Additionally, all three dioxides (TiO_2, ZrO_2,[56] HfO_2) are known CO_2 adsorbents. A two-metal approach should also be considered.

3.2 *The effect of halogen ligands*

All four water-free titanium oxy dihalides ($TiOX_2$, X = F, Cl, Br, I) as well as their complexes with electron donors have been reported,[57] along with several vanadium oxychlorides. A synopsis on $TiOCl_2$ chemistry has been presented in the introduction. $TiOF_2$ in the form of nanotubes has already been applied in photocatalytic hydrogen evolution.[58] Bromine and chlorine have been mentioned in co-doping of TiO_2, enhancing photocatalytic activity.[59] The halide effect, especially replacing $TiOCl_2$ with $TiOF_2$, $TiOBr_2$, or even $TiO(N_3)_2$ in our photocatalytic system, should be investigated in detail.

3.3 *The quest for efficient photoactive organic ligands*

The essential role of the PI ligand in the operation of our AP system has been analyzed. Most remarkable is the presence of PI in numerous titanium complexes, revealing the pathway of each individual step in the continuous operation of our visible light photocatalytic system. The observed parallel PI oligomerization reaction could be a concern, by depriving the system of the PI ligand and gradually weakening the system's intrinsic efficiency. One remedy to avoid PI oligomerization could be the blockage of the indole framework C_3 position, where the oligomerization bonding occurs, by substitution, for example, using 2,3-diphenyl indole as the ligand. Another option would be the use of other common indole derivatives, such as indigo dye.

Taking advantage of the photocatalytic phosphine- and phosphine oxide water activation for radical hydrogenation,[60] we may prepare the mixed PI·Ph_3PO·$TiCl_4$ complex **58**, which upon hydrolysis is expected to form complexes **59** and **60** (Figure 29), with enhanced photocatalytic radical hydrogenation capabilities.

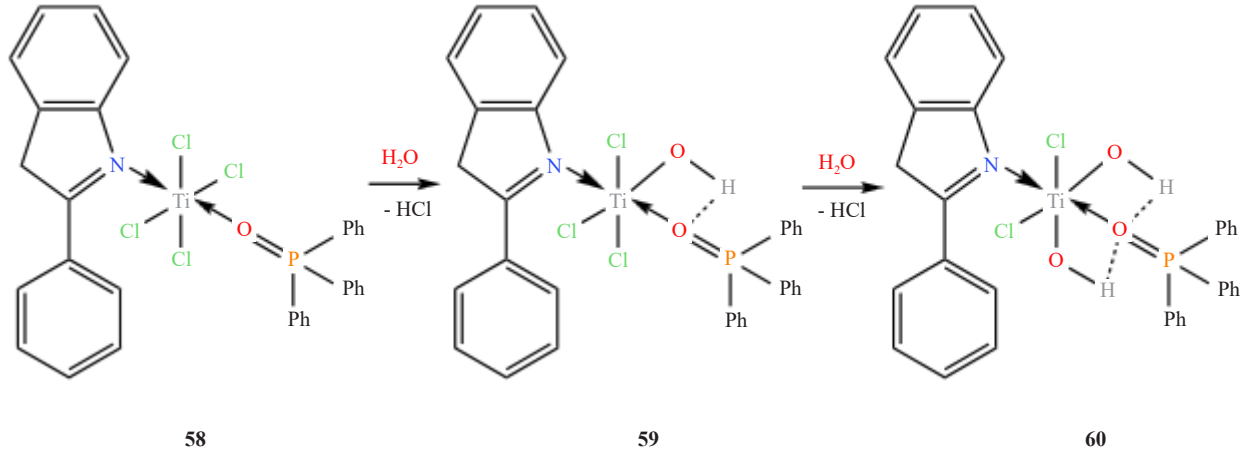

Figure 29. Mixed PI·Ph_3PO·$TiCl_4$ complex **58** and hydrolyzed complexes **59** and **60** expected to show enhanced water activation for radical hydrogenation

Known ligands of photon-absorbing ruthenium, rhenium, cobalt, and other metal complexes could be attractive candidates for the preparation of $TiOX_2$ or even $TiSX_2$-based photocatalysts. Notably, 2,2'-bipyridine and derivatives with electron-withdrawing groups at 5,5'-positions,[61] pyridylpyrazole,[62] and N_2,N_6-bis-(diphenylphosphanyl)-N_2,N_6-diphenylpyridine-2,6-diamine[63] are among the ligands we strongly recommend.

4. Experimental section

Materials and Procedures. 2-Phenyl indole 99% (PI), $TiCl_4$, and toluene 99.5% were purchased from a commercial source and used as received. Toluene was dried using 3A molecular sieves. Stock solutions were prepared of a 0.2 M $TiCl_4$ in toluene and a 0.138 M (saturated at ambient temperature) PI solution also in toluene.

Preparation of the 2:1 PI/$TiCl_4$ Complex. The experiment was carried-out in a dry-box under dry N_2. Into a 500 ml Erlenmeyer flask equipped with a magnetic stirrer, 100 ml of a 0.138 M PI in toluene solution (saturated at room temperature) was transferred. To the stirred solution, 34.5 ml of a 0.2 M $TiCl_4$ in toluene solution was added dropwise at room temperature. The resulting dark brown precipitate (3.52 g) was filtered in open air, then charged to a 50 ml glass vial tightly sealed for three weeks. The vial was exposed in a horizontal position to visible light at an average room temperature of 24 °C. During exposure, the color of the solid within the vial changed from dark brown to khaki, with surface areas of green, as shown in photo Figure 6.

Preparation of the 1:1 and 1:2 PI/$TiCl_4$ Complexes. These complexes were prepared following the same

procedure as the 2 : 1 complex. For the 1 : 1 PI/$TiCl_4$ complex, 69 ml of a 0.2 M $TiCl_4$ in toluene solution was added dropwise to 100 ml of a 0.138 M PI in toluene solution. For the 1 : 2 PI/$TiCl_4$ complex, 103.5 ml of a 0.2 M $TiCl_4$ in toluene solution was added dropwise to 100 ml of a 0.138 M PI in toluene solution. The products were filtered, transferred to 50 ml glass containers, and exposed to visible light as described above.

Analytical techniques

MALDI-TOF MS Spectra: Recorded with a Bruker instrument run with Daltonics autoflexR maX Analysis software. Solid samples chosen for analysis were dissolved in THF and CH_2Cl_2.

^{1}H and ^{13}C NMR Spectra: Recorded with a Bruker AvanceCore NMR 400 MHz instrument.

FTIR Spectra: Recorded with a Perkin Elmer Spectrum Two instrument with an ATR diamond crystal.

Author contributions

This manuscript was written by GGA with contributions from both authors. GGA suggested this study and interpreted the experimental data. MP performed the experimental work and chose the analytical tools.

Conflict of interest

The authors declare no competing financial interest.

References

[1] Gentle, K.; Somasundar, A.; Bhide, A.; Sen, A. Chemically powered synthetic "living" systems. *Chem*. **2020,** *6*(9), 2174-2185.

[2] Machin, A.; Cotto, M.; Duconge, J; Marquez, F. Artificial photosynthesis: Current advancements and future prospects. *Biomimetics* **2023,** *8*(1), 298-341.

[3] Kitano, M.; Tsujimaru, K.; Anpo, M. Hydrogen production using highly active titanium oxide-based photocatalysts. *Top. Catal*. **2008,** *49*(1), 4-17.

[4] Orsted. The Power of American Green Hydrogen. https://us.orsted.com › ørsted › north-america (accessed April 2, 2024).

[5] Sanz-Perez, E. S.; Murdock, C. R.; Didas, S. A.; Jones, C. W. Direct capture of CO_2 from ambient air. *Chem. Rev*. **2016,** *116*(19), 11840-11876.

[6] Nakajima, T.; Tamaki, Y.; Ueno, K.; Kato, E.; Noshikawa, T.; Ohkubo, K.; Yamazaki, Y.; Morimoto, T.; Ishitani, O. Photocatalytic reduction of low concentration of CO_2. *J. Am. Chem. Soc*. **2016,** *138*(42), 13818-13821.

[7] Hashimoto, K.; Irie, H.; Fujishima, A. TiO_2 photocatalysis: A historical overview and future prospects. *Japan J. Appl. Phys*. **2005,** *44*(12), 8269-8285.

[8] Eidsvag, H.; Bentouba, S.; Vajeeston, P.; Yohi, S.; Velauthapillai, D. TiO_2 as a photocatalyst for water splitting - An experimental and theoretical review. *Molecules* **2021,** *26*(7), 1687-1727.

[9] Ur Rehman, Z.; Bilal, M.; Hou, J.; Butt, F. K.; Ahmad, J.; Ali, S.; Hussein, A. Photocatalytic CO_2 reduction using TiO_2 z-scheme heterojunction composites: A review. *Molecules* **2022,** *27*(7), 2069-2111.

[10] Testino, A.; Bellobono, I. R.; Buscaglia, V.; Canevali, C.; D'Arienzo, M.; Polizzi, S.; Scotti, R.; Morazzoni, F. Optimizing the photocatalytic properties of hydrothermal TiO_2 by the control of phase composition and particle morphology. A systematic approach. *J. Am. Chem. Soc*. **2007,** *129*(12), 3564-3575.

[11] Park, H.; Goto, T.; Cho, S.; Nishida, H.; Sekino, T. Enhancing visible light absorption of yellow-colored peroxo-titanate nanotubes prepared using peroxo titanium complex ions. *ACS Omega* **2020,** *5*(37), 21753-21761.

[12] Lai, Q.; Toan, S.; Assiri, M. A.; Cheng, H.; Russel, A. G.; Adidharma, H.; Radosz, M.; Fan, M. Catalyst-$TiO(OH)_2$ could drastically reduce the energy consumption of CO_2 capture. *Nat. Commun*. **2018,** *9*(1), 2672.

[13] Wang, X.; Andrews, L. Infrared spectra and structures for group 4 dihydroxide and tetrahydroxide molecules. *J.*

Phys. Chem. A **2005,** *109*(48), 10689-10701.
[14] Andreiadis, E. S.; Chavarot-Kerlidou, M.; Fontecave, M.; Artero, V. Artificial photosynthesis: From molecular catalysts for light-driven water splitting to photoelectrochemical cells. *Photochem. Photobiol*. **2011,** *87*(5), 946-954.
[15] Godemann, C.; Dura, L.; Hollmann, D.; Grabow, K.; Bentrup, U.; Jiao, H.; Schulz, A.; Brückner, A.; Beweries, T. Highly selective visible light-induced Ti-O bond splitting in ansa-titanocene dihydroxido complex. *Chem. Commun*. **2015,** *51*(14), 3065-3068.
[16] Juliá, F. Ligand-to-metal charge transfer (LMCT) photochemistry at 3d-metal complexes: An emerging tool for sustainable organic synthesis. *ChemCatChem* **2022,** *14*(19), e202200916.
[17] Yang, S.-M.; Yu, T.-M.; Huang, H.-P.; Ku, M.-Y.; Tseng, S.-Y.; Tsai, C.-L.; Chen, H.-P.; Hsu, L.; Liu, C.-H. Light-driven manipulation of picobubbles on a titanium oxide phthalocyanine-based optoelectronic chip. *Appl. Phys. Lett*. **2011,** *98*(15), 153512.
[18] Dehnicke, K. Titan(IV)-Oxichlorid $TiOCl_2$. *ZAAC* **1961,** *309*(1-2), 266.
[19] Fowless, G. W. A.; Lewis, D. F.; Walton, R. A. The reactivity of titanium(IV) oxide dichloride towards nitrogen and oxygen donor molecules and a study of the complex anions $TiOCl_4^{2-}$ and $TiOCl_5^{2-}$. *J. Chem. Soc. A* **1968,** 1468-1473.
[20] Feltz, A. Untersuchungen über chlorverbindungen der IV. Gruppe. I. Über ein durch Solvatation stabilisiertes Titan (IV)-oxidchlorid, Ti_2Cl_6O [Investigations on chlorine compounds of group IV. I. On a titanium (IV) oxide chloride stabilized by solvation, Ti_2Cl_6O]. *ZAAC* **1963,** *323*(1-2), 35-43.
[21] Arzoumanidis, G. G. In *Direct Metallation of 2-Phenyl-1H-Indole (PI) with MCl_4 (M=Ti, Zr). Effect of the PI Molar Ratio on the Formation of Two Different Metallated Complexes*, ACS Spring Meeting, 2021.
[22] Arzoumandis, G.; Chamot. E. Direct otho-metallation of aryl substituted ligands with $TiCl_4$ and $ZrCl_4$. An experimental and DFT study with 2-phenyl indole as the ligand. *ChemRxiv* **2019**.
[23] Yamauchi, O.; Takani, M.; Toyoda, K.; Masuda, H. Indole nitrogen-palladium(II) bonding. Chemical and structural characterization of palladium(II) complexes of alkylindoles and intermediacy of the 3H-indole ring. *Inorg. Chem*. **1990,** *29*(10), 1856-1860.
[24] Liu, X.; Yang, D.; Liu, Z.; Wang, Y.; Liu, Y.; Wang, S.; Wang, P.; Cong, H.; Chen, Y.-H.; Lu, L.; Qi, X.; Yi, H.; Lei, A. Unraveling the structure and reactivity pattern of the indole radical cation in regioselective electrochemical oxidative annulations. *J. Am. Chem. Soc*. **2023,** *145*(8), 3175-3186.
[25] Goryo, S.; Iwata, K. Photoionization of 3-methylindole embedded in sodium dodecyl sulfate and dodecylmethylammonium chloride micelles: Migration of electrons generated in micelle cores and their solvation in outside water. *J. Phys. Chem. Lett*. **2023,** *14*(6), 1479-1484.
[26] Walden, S. E.; Wheeler, R. A. Distinguishing features of indolyl radical and radical cation: Implications for tryptophan radical studies. *J. Phys. Chem*. **1996,** *100*(4), 1530-1535.
[27] Peon, J.; Hess, G. C.; Pecourt, J.-M. L.; Yazawa, T.; Kohler, B. Ultrafast photoionization dynamics of indole in water. *J. Phys. Chem. A* **1999,** *103*(14), 2460-2466.
[28] Muneer, M.; Saquib, M.; Oamar, M.; Behnemann, D. Photocatalyzed reaction of indole in an aqueous suspension of titanium dioxide. *Res. Chem. Intermed*. **2010,** *36*(1), 121-125.
[29] Wang, L. Ligand modification strategies for mononuclear water splitting catalysts. *Front. Chem*. **2022,** *10*, 996386.
[30] Bailey, G. A.; Fogg, D. E. Confronting neutrality: Maximizing success in the analysis of transition-metal catalysts by MALDI mass spectrometry. *ACS Catal*. **2016,** *6*, 4962-4971.
[31] Dopke, N. C.; Treichel, P. M.; Vestling, M. M. Matrix-assisted laser desorption/ionization time-of-flight mass spectroscopy (MALDI-TOF MS) of Rhenium(III) halides: A characterization tool for metal atom clusters. *Inorg. Chem*. **1998,** *37*(6), 1272-1277.
[32] KingDraw. http://kingdraw.com (accessed April 2, 2024).
[33] Wang, T.-H.; Navarrete-Lopez, A. M.; Li, S.; Dixon, D. A.; Gole, J. L. Hydrolysis of $TiCl_4$: Initial steps in the production of TiO_2. *J. Phys. Chem. A* **2010,** *114*(28), 7561-7570.
[34] Kumar, A.; Bhardwaj, R.; Mandal, S. K.; Choudhury, J. Transfer hydrogenation of CO_2 and CO_2 derivatives using alcohols as hydride sources: Bonding an H_2-free alternative strategy. *ACS Catal*. **2022,** *12*, 8886-8903.
[35] Kaithal, A.; Hölscher, M.; Leitner, W. Catalytic hydrogenation of cyclic carbonates using manganese complexes. *Angew. Chem., Int. Ed*. **2018,** *130*, 13637-13641.
[36] Fan, Y.; Bao, J.; Shi, L.; Li, S.; Lu, Y.; Liu, H.; Wang, H.; Zhong, L.; Sun, Y. Photocatalytic coupling of methanol and formaldehyde into ethylene glycol with high atomic efficiency. *Catal. Lett*. **2018,** *148*, 2274-2282.
[37] Flores, L. A.; Murphy, J. G.; Copeland, W. R.; Dixon, D. A. Reaction of CO_2 with groups 4 and 6 transition metal

oxide clusters. *J. Phys. Chem. A* **2017,** *121*, 8719-8727.
[38] Nguyen, T. P.; Nguyen, D. L. T.; Nguyen, V.-H.; Le, T.-H.; Vo, D.-V. N.; Trinh, Q. T.; Bae, S.-R.; Chae, S. Y.; Kim, S. Y.; Le, Q. V. Recent advances in TiO_2-based photocatalysts for reduction of CO_2 to fuels. *Nanomaterials* **2020,** *10*, 337-360.
[39] Special Database for Organic Compounds (SDBS). UC Santa Barbara. https://www.library.ucsb.edu (accessed April 2, 2024).
[40] Song, H.; Guo, H. Mode specificity in the HCl + OH → Cl + H_2O reaction: Polanyi's rules vs sudden vector projection model. *J. Phys. Chem. A* **2015,** *119*(5), 826-831.
[41] Van Tamelen, E. E.; Fechter, R. B.; Schneider, S. W.; Boche, G.; Greeley, R. H.; Akermark, B. Titanium(II) in the fixation-reduction of molecular nitrogen under mild conditions. *J. Am. Chem. Soc*. **1969,** *91*(6), 1551-1552.
[42] Reinholdt, A.; Pividori, D.; Laughlin, A. L.; DiMucci, I. M.; MacMillan, S. N.; Jafari, M. G.; Gau, M. R.; Carroll, P. J.; Krzystek, J.; Ozarowski, A.; Telser, J.; Lancaster, K. M.; Meyer, K.; Mindola, D. J. A mononuclear and high-spin tetrahedral TiII complex. *Inorg. Chem*. **2020,** *59*, 17834-17850.
[43] Pan, H.; Heagy, M. D. Photons to formate: A review on photocatalytic reduction of CO_2 to formic acid. *Nanomaterials* **2020,** *10*, 2422-2445.
[44] Rosko, M. C.; Espinoza, E. M.; Arteta, S.; Kromer, S.; Wheeker, J. P.; Castelliano, F. N. Employing long-range inductive effects to modulate metal-to ligand charge transfer photoluminescence in homoleptic Cu(I) complexes. *Inorg. Chem*. **2023,** *62*, 3248-3259.
[45] Avyappan, R.; Abdaighani, I.; Da Costa, R. C.; Owen, G. R. Recent developments on the transformation of CO_2 utilizing ligand cooperation and related strategies. *Dalton Trans*. **2022,** *51*, 11582-11611.
[46] Fachinetti, G.; Floriani, C.; Chesi-Villa, A.; Guastini, C. Carbon dioxide activation: Deoxygenation and disproportionation of carbon dioxide promoted by Bis(cyclopentadienyl)titanium and-zirconium derivatives. A novel bonding mode of the carbonato and a trimer of the zirconyl unit. *J. Am. Chem. Soc*. **1979,** *150*, 1767-1775.
[47] Del Bene, J. E.; Alkorta, I.; Alquero, H. Carbenes as electron-pair donors to CO_2 for C···C tetrel bonds and C-C covalent bonds. *J. Phys. Chem. A* **2017,** *20*, 4039-4047.
[48] Burlakov, V. V.; Dolgushin, F. M.; Struchov, Y. T.; Shur, V. B.; Rosenthal, U.; Thewalt, U. Interaction of carbon dioxide with the bis(trimethylsilyl)acetylene complex of permethyltitanocene: synthesis and structure of the binuclear carbonate complex $(Cp_2*Ti)_2CO_3$. *J. Organom. Chem*. **1996,** *522*, 241-247.
[49] Papai, I.; Masketti, J.; Fournier, R. Theoretical study of the Ti atom with CO_2: Cleavage of the C-O bond. *J. Phys. Chem. A* **1997,** *101*, 4465-4471.
[50] Kong, X.; Zeng, C.; Wang, X.; Huang, J.; Li, C.; Fei, J.; Li, J.; Feng, O. Ti-O-O coordination bond caused visible light photocatalytic property of layered titanium oxide. *Sci. Rep*. **2016,** *6*, 29049.
[51] Funes-Ardoiz, I.; Maseras, F. Oxidative coupling mechanisms: Current state of understanding. *ACS Catal*. **2018,** *6*, 1161-1172.
[52] Couturier-Tamburelli, J. P.; Aycard, M. W.; Wong, M. W.; Wentrup, C. A stable ketene-pyridine prereactive intermediate: Experimental and theoretical identifications of the C_3O_2···pyridine complex. *J. Phys. Chem*. **2000,** *104*, 3466-3471.
[53] Liu, D-J. Electrochemical conversion of CO_2 to long-chain hydrocarbons. *Joule* **2022,** *6*, 1978-1980.
[54] Udum, Y. A.; Düdüksü, M.; Köleli, F. Electrochemical polymerization and spectroscopic investigation of 2-methyl indole. *React. Funct. Polym*. **2008,** *68*, 861-867.
[55] Sivaram, V. The *Race to Invent the Artificial Leaf. In Taming the Sun: Innovations to Harness Solar Energy and Power the Planet*; MIT Press, 2018.
[56] Pokrovski, K.; Jung, K. T.; Bell, A. T. Investigation of CO and CO_2 adsorption on tetragonal and monoclinic zirconia. *Langmuir* **2001,** *17*(14), 4297-4303.
[57] Walton, R. A. Halides and oxyhalides of the early transition series and their stability and reactions in nonaqueous media. In *Progress in Inorganic Chemistry*; Lippard, S. J., Ed.; John Willey & Sons, 1972; Vol. 16, pp 8.
[58] Ilango, P. R.; Huang, H.; Li, L.; Yang, S.; Peng, S. Facile synthesis of self-organized single crystalline $TiOF_2$ nanotubes for photocatalytic hydrogen evolution. *Solid State Sci*. **2021,** *117*, 106627.
[59] Luo, H.; Takata, T.; Lee, Y.; Zhao, J.; Domen, K.; Yan, Y. Photocatalytic activity enhancing for titanium dioxide by co-doping with bromine and chlorine. *Chem. Mater*. **2004,** *16*(5), 846-849.
[60] Zheng, J.; Mück-Lichtenfeld, C.; Studer, A. Photocatalytic phosphine-mediated water activation for radical hydrogenation. *Nature* **2023,** *619*, 506-514.
[61] Fenton, T. G.; Louis, M. E.; Li, G. Effect of ligand derivation at different positions on photochemical properties of hybrid Re(I) photocatalysts. *J. Mol. Catal. A: Chem*. **2016,** *411*, 272-278.

[62] Merillas, B.; Cuellar, E.; Diez-Varga, A.; Asensio-Bartolome, M.; Garcia-Herbosa, G.; Torroba, T.; Martin-Alvarez, J. M.; Miguel, D.; Villafane, F. Whole microwave synthesis of pyridylpyrazole and of Re and Ru luminescent pyridylpyrazole complexes. *Inorg. Chim. Acta* **2019,** *484*, 1-7.
[63] Kinzel, N. W.; Demirbas, D.; Bill, E.; Wehermüller, T.; Werle, C.; Kaeffer, N.; Leitner, W. Systematic variation of 3d metal centers in a redox-innocent ligand environment: Structures, electrochemical properties, and carbon dioxide activation. *Inorg. Chem*. **2021,** *60*, 19062-19078.